

Causal View of Time Series Imputation: Some Identification Results on Missing Mechanism

Ruichu Cai^{1,2}, Kaitao Zheng¹, Junxian Huang¹, Zijian Li^{3*}, Zhengming Chen¹,
Boyan Xu¹ and Zhifeng Hao⁴

¹School of Computer Science, Guangdong University of Technology, Guangzhou 510006, China

²Peng Cheng Laboratory, Shenzhen 518066, China

³Mohamed bin Zayed University of Artificial Intelligence, Masdar City, Abu Dhabi

⁴College of Science, Shantou University, Shantou 515063, China

cairuichu@gmail.com, zhengkaitao142857@qq.com,

{huangjunxian459, leizigin, chenzhengming1103, hpakyim}@gmail.com, haozhifeng@stu.edu.cn

Abstract

Time series imputation is one of the most challenge problems and has broad applications in various fields like health care and the Internet of Things. Existing methods mainly aim to model the temporally latent dependencies and the generation process from the observed time series data. In real-world scenarios, different types of missing mechanisms, like MAR (Missing At Random), and MNAR (Missing Not At Random) can occur in time series data. However, existing methods often overlook the difference among the aforementioned missing mechanisms and use a single model for time series imputation, which can easily lead to misleading results due to mechanism mismatching. In this paper, we propose a framework for time series imputation problem by exploring **Different Missing Mechanisms (DMM** in short) and tailoring solutions accordingly. Specifically, we first analyze the data generation processes with temporal latent states and missing cause variables for different mechanisms. Sequentially, we model these generation processes via variational inference and estimate prior distributions of latent variables via normalizing flow-based neural architecture. Furthermore, we establish identifiability results under the nonlinear independent component analysis framework to show that latent variables are identifiable. Experimental results show that our method surpasses existing time series imputation techniques across various datasets with different missing mechanisms, demonstrating its effectiveness in real-world applications.

1 Introduction

While data-driven deep models have achieved significant performance on time series analysis [Tang and Matteson, 2021; Wu *et al.*, 2022] and massive applications, like traffic [Jiang

et al., 2023; Cai *et al.*, 2025a], weather [Wu *et al.*, 2023], and the Internet of Things [Cai *et al.*, 2025b], their properties usually require complete data. However, the missing values of time series led by sensor failures hinder the deployment of existing algorithms to real-world scenarios. To address this challenge, time series imputation [Nie *et al.*, 2023; Fang *et al.*, 2023] is proposed. The primary goal of time series imputation is to leverage the observed data and the missing indicators to identify the distribution of time series data.

To identify the distribution from the time series data [Li *et al.*, 2025], different approaches have been proposed to identify the distribution from the time series data with missing values [Li *et al.*, 2024b]. Previously, researchers used statistical tools [Acuna and Rodriguez, 2004; Van Buuren and Groothuis-Oudshoorn, 2011] to address the time series imputation. Recent methods based on deep neural networks can be categorized into the predictive and the generative methods. For example, the predictive models harness different neural architectures like recursive neural networks [Cao *et al.*, 2018; Che *et al.*, 2018], convolution neural networks [Wu *et al.*, 2022], and Transformer [Nie *et al.*, 2023; Liu *et al.*, 2023b] to model the inherent dependencies of among variables. Additionally, the generative methods use varied deep generative models like variational autoencoders (VAE) [Choi and Lee, 2023; Fortuin *et al.*, 2020; Cai *et al.*, 2025c], generative adversarial networks (GANs) [Luo *et al.*, 2018; Zhang *et al.*, 2021], and diffusion models [Alcaraz and Strodthoff, 2022; Tashiro *et al.*, 2021; Chen *et al.*, 2023] to model the distribution of complete time series data. In summary, these methods model the temporal latent process and generation from latent to observed variables for missing value imputation. Please refer to Appendix A for related work on time series imputation and identification of the temporal latent process.

In practical applications, time series data can be affected by various types of missing data mechanisms, such as MCAR (Missing Completely At Random), MAR (Missing At Random), and MNAR (Missing Not At Random). While current methods have achieved success in time series imputation, they often employ a single model that does not account for the differences between these mechanisms. Given an example in healthcare that follows the MNAR mechanisms, patients who

*corresponding author: leizigin@gmail.com

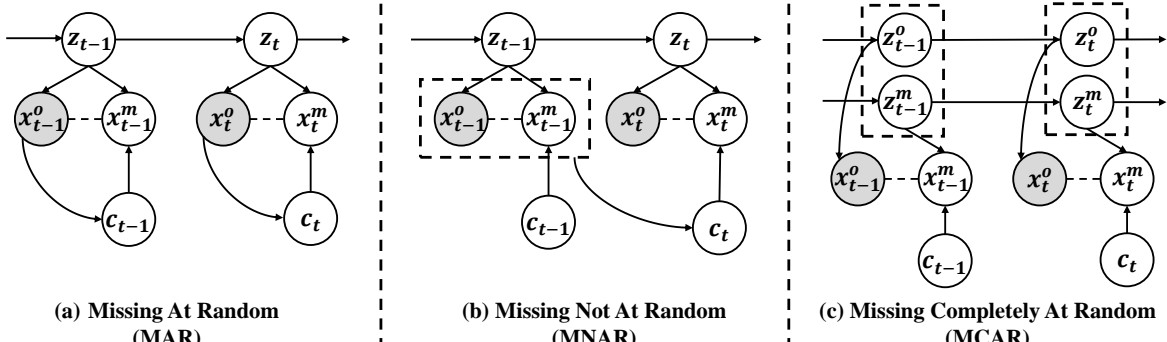


Figure 1: Data generation processes of time series data under different missing mechanisms. z_t are temporal latent variables that describe the temporal dependencies. x_t^o are the observed variables, x_t^m are the missing data and c_t denotes the missing cause variables. (a) The data generation process under the missing at random mechanism, where missingness is related to the observed data but not the unobserved data. (b) The data generation process under the missing not at random mechanism, where the missingness is influenced by the observed data and missing data in the previous time step. (c) The data generation process under the missing completely at random mechanism, where missing data is led by random issues, and the latent missing variables can be considered as random noises.

experience worsening conditions may not return for scheduled follow-ups, resulting in missing data for the later stages of the treatment. In this case, if a model uses a mismatched missing mechanism like MCAR and ignores the dependency between the missing format and the observed values, it is hard for it to achieve an accurate imputation performance. Therefore, it is essential for time series imputation to model the time series data according to different missing mechanisms.

To better exploit the missing mechanisms, we explore **Different Missing Mechanisms** and propose the corresponding methods, forming a general framework named **DMM**. We first analyze the data generation processes of time series data under different missing mechanisms, including Missing At Random (MAR), Missing Not At Random (MNAR), and Missing Completely At Random (MCAR). [Locatello *et al.*, 2019] find that the MCAR mechanism is not identifiable and rare in real-world scenarios. Based on the aforementioned data generation processes, we employ variational inference to model how missing data are generated and the normalizing flow-based neural architectures to enforce the identification of latent variables. Moreover, we analyze the identification results for different missing mechanisms, in which the temporal latent variables and latent missing causes can be identified in the case of MAR and MNAR. Our approach is validated through massive semisynthetic datasets on all the missing mechanisms, the experimental results show that our DMM method outperforms the state-of-the-art baselines. Please refer to Appendix D for more details on missing mechanism.

2 Preliminaries

In this paper, we focus on the time series imputation problem in the presence of various types of missing mechanisms. We first formalize the generation process for the time series imputation problem, and then introduce a graphical model (termed *imputation m-graphs*) to represent it.

Data-generating process. We first let the time series data $X = \{x_1, x_2, \dots, x_T\}$, $x_t \in \mathbb{R}^n$ are generated from latent variables $z_t \in \mathcal{Z} \subseteq \mathbb{R}^n$ by an invertible and nonlinear mixing function g as shown in Equation (1):

$$x_t = g(z_t) \quad (1)$$

Moreover, the i -th dimension latent variable $z_{t,i}$ is time-delayed and causally related to the historical latent variables $z_{t-\tau}$ with the time lag τ via a nonparametric function f_i , which is shown as in Equation (2).

$$z_{t,i} = f_i(z_{t-\tau,k} | z_{t-\tau,k} \in \mathbf{Pa}(z_{t,i}), \epsilon_{t,i}) \quad \text{with} \quad \epsilon_{t,i} \sim p_{\epsilon_{t,i}}, \quad (2)$$

where $\mathbf{Pa}(z_{t,i})$ denotes the set of latent variables that directly cause $z_{t,i}$ and $\epsilon_{t,i}$ denotes the temporally and spatially independent noise extracted from a distribution $P_{\epsilon_{t,i}}$. Here, we provide a medical example to explain this data generation process. First, we let x_t be the measurable index like body temperature or blood pressure. And then z_t can be considered as the virus concentration, which is hard to measure.

Graphical Notation. To describe the time series data with missing values, given an entire time series data x_t , we further partition the time series data into the observed variables x_t^o and missing variables x_t^m , such that $x_t = x_t^o \cup x_t^m$. To model the generation process x_t , we use the missing graph with imputation problems (abbreviated as *imputation m-graphs*) such that x_t can be represented by a causal graph, where the gray nodes represent observed variables, and the white nodes represent unobserved variables. Note that this graph differs from the m-graph [Mohan *et al.*, 2013], where, in the imputation m-graph, the missing variable is determined by its cause variables. Since the direct causal relationships between observed and missing variables are unknown (e.g., the edge between x_t^o and x_t^m exist or not), we use dashed lines to represent these uncertain connections. Based on the imputation m-graph, one can easily distinguish different missing mechanisms for the imputation problem, leading to more general identifiability results (See the identification results section).

Objectives. In the context of time series imputation, we assume that the existence of a training set $\{X_i^o, X_i^m\}_{i=1}^M$ with the size of M . While in the I.I.D test set, we can only access $\{X_i^o\}_{i=1}^T$ with the size of T , our *goal* is to use the training dataset to obtain a model, such that it can identify the distribution $P(X^o, X^m)$ of test data.

As mentioned above, existing methods may suffer from mechanism mismatching problems since they usually use one

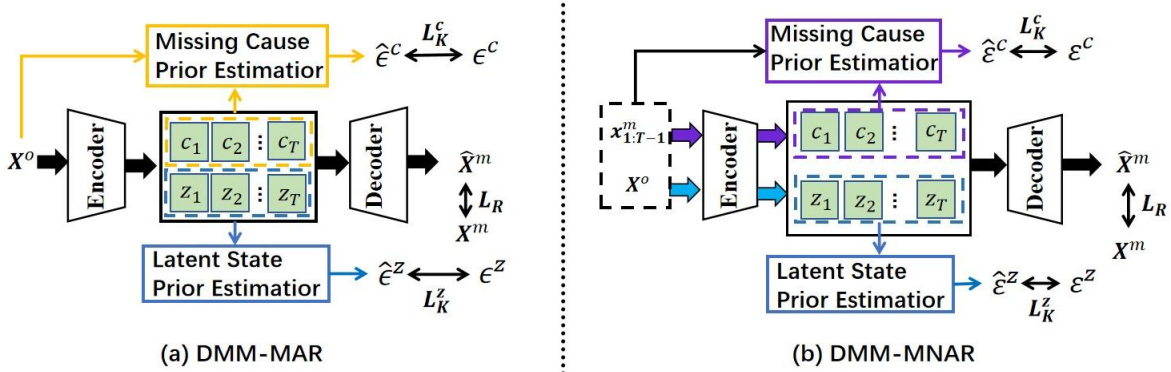


Figure 2: Illustration of the DMM framework. X^o are the observed variables, X^m are the missing data. The latent state variables $\mathbf{z}_{1:T}$ and the missing cause variables $\mathbf{c}_{1:T}$ are extracted from the encoder. The latent state and missing cause prior networks for DMM-MAR and DMM-MNAR are used to estimate the prior distributions.

model to cover all the missing mechanisms, making it hard to identify the distribution $P(X^o, X^m)$. In general, all missing data problems fall into one of the following mechanisms [Rubin, 1976]: missing completely at random (MCAR), missing at random (MAR), and missing not at random (MNAR). Fortunately, with the imputation m-graph, these missing mechanisms can be precisely categorized by incorporating the missing cause variables \mathbf{c}_t , which are introduced as follows.

2.1 Missing At Random

When data are **Missing At Random** (MAR), the missingness is related to known variables but not to the values that are missing. Specifically, the missing cause variables are influenced by the observed variables, and they further lead to the missingness. Suppose the time series data are generated by the latent process shown in Eq. (1) and Eq. (2), the MAR missingness can be further represented by Figure 1(a), where the missing cause variables \mathbf{c}_t ($\mathbf{c}_t \rightarrow \mathbf{x}_t^m$) are influenced by the observed variable \mathbf{x}_t^o (i.e., $\mathbf{x}_t^o \rightarrow \mathbf{c}_t$). The dashed edge in Figure 1(a) between \mathbf{x}_t^m and \mathbf{x}_t^o indicates that we allow a direct causal relationship between them.

By combining the generating process and Figure 1 (a), the joint distribution in MAR can be formalized as:

$$p(\mathbf{x}_{1:T}^o, \mathbf{x}_{1:T}^m) = \int_{\mathbf{c}_{1:T}} \int_{\mathbf{z}_{1:T}} P(\mathbf{x}_{1:T}^m | \mathbf{c}_{1:T}, \mathbf{z}_{1:T}, \mathbf{x}_{1:T}^o) P(\mathbf{z}_{1:T} | \mathbf{x}_{1:T}^o) P(\mathbf{c}_{1:T} | \mathbf{x}_{1:T}^o) P(\mathbf{x}_{1:T}^o) d\mathbf{c}_{1:T} d\mathbf{z}_{1:T}, \quad (3)$$

where $\mathbf{z}_{1:T} := \{\mathbf{z}_1, \dots, \mathbf{z}_T\}$ and $\mathbf{c}_{1:T} := \{\mathbf{c}_1, \dots, \mathbf{c}_T\}$. In this case, we can identify the joint distribution by modeling 1) generative model $P(\mathbf{x}_{1:T}^m | \mathbf{c}_{1:T}, \mathbf{z}_{1:T}, \mathbf{x}_{1:T}^o)$ of missing values; 2) the conditional distributions of missing cause and latent variables, i.e., $P(\mathbf{c}_{1:T} | \mathbf{x}_{1:T}^o)$ and $P(\mathbf{z}_{1:T} | \mathbf{x}_{1:T}^o)$.

Establishing the joint distribution for MAR allows us to perform accurate variational inference to recover the distribution $p(\mathbf{z}_t)$ and $p(\mathbf{c}_t)$, and identify $P(X^o, X^m)$ accordingly (see implementation section).

2.2 Missing Not At Random

When data are **Missing Not At Random** (MNAR), the missingness depends on unobserved data. Specifically, the missing causes are influenced by the historical missing variables,

and they further lead to the current missingness. Suppose the time series data are generated by the latent process shown in Eq. (1) and Eq. (2), the MNAR missingness can be further described by Figure 1(b), where the missing causes \mathbf{c}_t ($\mathbf{c}_t \rightarrow \mathbf{x}_t^m$) are influenced by historical missing variables \mathbf{x}_{t-1}^o and \mathbf{x}_{t-1}^m , i.e., $\mathbf{x}_{t-1}^o \rightarrow \mathbf{c}_t \& \mathbf{x}_{t-1}^m \rightarrow \mathbf{c}_t$. The dashed box in Figure 1(b) means that both \mathbf{x}_{t-1}^o and \mathbf{x}_{t-1}^m are causes of \mathbf{c}_t . Similarly, based on the corresponding imputation m-graph, the joint distribution can be formalized as:

$$\begin{aligned} & p(\mathbf{x}_{1:T}^o, \mathbf{x}_{1:T}^m) \\ &= \int_{\mathbf{c}_{1:T}} \int_{\mathbf{z}_{1:T}} P(\mathbf{x}_{1:T}^o, \mathbf{x}_{1:T}^m, \mathbf{c}_{1:T}, \mathbf{z}_{1:T}) d\mathbf{c}_{1:T} d\mathbf{z}_{1:T} \\ &= \int_{\mathbf{c}_{1:T}} \int_{\mathbf{z}_{1:T}} P(\mathbf{x}_1^m | \mathbf{c}_1, \mathbf{z}_1, \mathbf{x}_1^o) P(\mathbf{z}_1 | \mathbf{x}_1^o) P(\mathbf{c}_1) P(\mathbf{x}_1^o) \\ & \quad \prod_{t=2}^T P(\mathbf{x}_t^m | \mathbf{c}_t, \mathbf{z}_t, \mathbf{x}_t^o) P(\mathbf{z}_t | \mathbf{x}_t^o) P(\mathbf{c}_t | \mathbf{x}_{t-1}^o) P(\mathbf{x}_t^o) d\mathbf{c}_{1:T} d\mathbf{z}_{1:T}, \end{aligned} \quad (4)$$

where $\mathbf{z}_{1:T} := \{\mathbf{z}_1, \dots, \mathbf{z}_T\}$ and $\mathbf{c}_{1:T} := \{\mathbf{c}_1, \dots, \mathbf{c}_T\}$. In this case, we can identify the joint distribution by modeling 1) generative model $P(\mathbf{x}_t^m | \mathbf{c}_t, \mathbf{z}_t, \mathbf{x}_t^o)$ of missing values; 2) the conditional distributions of missing cause and latent variables, i.e., $P(\mathbf{c}_t | \mathbf{x}_{t-1}^o)$ and $P(\mathbf{z}_t | \mathbf{x}_t^o)$.

2.3 Missing Completely At Random

When data are **Missing Completely At Random** (MCAR), however, it is impossible to reconstruct the latent process and recover $p(\mathbf{x}_{1:T}^o, \mathbf{x}_{1:T}^m)$, since the missingness are independent of all other variables, as shown in Figure 1(c). In this case, distribution $p(\mathbf{x}_{1:T}^o, \mathbf{x}_{1:T}^m) = \int_{\mathbf{z}_{1:T}^o, \mathbf{z}_{1:T}^m, \mathbf{c}_{1:T}} p(\mathbf{x}_{1:T}^o | \mathbf{z}_{1:T}^o) p(\mathbf{x}_{1:T}^m | \mathbf{z}_{1:T}^m, \mathbf{c}_{1:T}) p(\mathbf{z}_{1:T}^o, \mathbf{z}_{1:T}^m, \mathbf{c}_{1:T}) d\mathbf{z}_{1:T}^o d\mathbf{z}_{1:T}^m d\mathbf{c}_{1:T}$ are not identifiable since it is hard to identify $p(\mathbf{z}_{1:T}^o, \mathbf{z}_{1:T}^m, \mathbf{c}_{1:T})$ without further auxiliary variables [Locatello *et al.*, 2019].

In real-world scenarios, this case is rare since complex relationships exist among latent variables, making that the observed and missing variables are not independent. Since the MCAR mechanism is rare in real-world scenarios, we mainly investigate the time series imputation problem under the MAR and MNAR scenarios.

3 Implementation of DMM Framework

Based on these data generation processes, we introduce the DMM framework as shown in Figure 2, which models the data generation process of MAR and MNAR mechanisms. Specifically, the DMM framework contains two models, which we name for MAR and MNAR mechanisms DMM-MAR and DMM-MNAR, respectively. Please refer to Appendix F for implementation details.

3.1 DMM-MAR model

The DMM-MAR model is shown in Figure 2(a), which is built on a variational inference neural architecture with prior estimators for latent states and missing cause variables.

Sequential Variational Backbone architecture for DMM-MAR. We effectively leverage the variational autoencoder to model the time series data. Specifically, for the data generation process of MAR, we have the following approach:

$$\begin{aligned} ELBO_A = & \underbrace{\mathbb{E}_{q(\mathbf{z}_{1:T}, \mathbf{c}_{1:T} | \mathbf{x}_{1:T}^o)} \ln p(\mathbf{x}_{1:T}^m | \mathbf{z}_{1:T}, \mathbf{c}_{1:T})}_{\mathcal{L}_R} \\ & - \underbrace{D_{KL}(q(\mathbf{z}_{1:T} | \mathbf{x}_{1:T}^o) || p(\mathbf{z}_{1:T}))}_{\mathcal{L}_K^z} \\ & - \underbrace{D_{KL}(q(\mathbf{c}_{1:T} | \mathbf{x}_{1:T}^o) || p(\mathbf{c}_{1:T}))}_{\mathcal{L}_K^c}, \end{aligned} \quad (5)$$

where D_{KL} denotes the KL divergence. Specifically, $q(\mathbf{z}_{1:T} | \mathbf{x}_{1:T}^o)$ and $q(\mathbf{c}_{1:T} | \mathbf{x}_{1:T}^o)$ denote the encoders for the latent states \mathbf{z}_t and missing cause variables \mathbf{c}_t , which are used to approximate the prior distribution. Technologically, these encoders can be formalized as follows:

$$\hat{\mathbf{z}}_{1:T} = \phi_{\mathbf{z}}^A(\mathbf{x}_{1:T}^o), \quad \hat{\mathbf{c}}_{1:T} = \phi_{\mathbf{c}}^A(\mathbf{x}_{1:T}^o), \quad (6)$$

where $\phi_{\mathbf{z}}^A$ and $\phi_{\mathbf{c}}^A$ ¹ denote the latent states encoder and the missing cause encoder, respectively. Moreover, $p(\mathbf{x}_{1:T}^m | \mathbf{z}_{1:T}, \mathbf{c}_{1:T})$ denote the decoder for missing value prediction, which is formalized as follows:

$$\hat{\mathbf{x}}_{1:T}^m = F_A(\hat{\mathbf{z}}_{1:T}, \hat{\mathbf{c}}_{1:T}), \quad (7)$$

where F_A denotes the predictor and it is implemented by Multi-layer Perceptron networks (MLPs).

3.2 Prior Estimator for Temporal Latent States and Missing Cause Variables

To model the prior distributions of temporal latent states and missing cause variables, we propose the latent state prior estimator and missing cause prior estimator, respectively.

As for the latent state prior estimator, we first let $\{r_i^A\}$ be a set of learned inverse transition functions that take the estimated latent variables and output the noise term, i.e., $\hat{\epsilon}_{t,i}^z = r_i^A(\hat{\mathbf{z}}_{t,i}, \hat{\mathbf{z}}_{t-1})$ and each r_i^A is modeled with MLPs. Then we devise a transformation $\psi_c^A := \{\hat{\mathbf{z}}_{t-1}, \hat{\mathbf{z}}_t\} \rightarrow \{\hat{\mathbf{z}}_{t-1}, \hat{\epsilon}_t^z\}$, and its Jacobian is $\mathbf{J}_{\psi_c^A} = \begin{pmatrix} \mathbb{I} & 0 \\ * & \text{diag}\left(\frac{\partial r_i^A}{\partial \hat{\mathbf{z}}_{t-1,i}}\right) \end{pmatrix}$, where $*$

denotes a matrix. By applying the change of variables formula, we have the following equation:

$$\ln p(\hat{\mathbf{z}}_{t-1}, \hat{\mathbf{z}}_t) = \ln p(\hat{\mathbf{z}}_{t-1}, \hat{\epsilon}_t^z) + \ln |\det(\mathbf{J}_{\psi_c^A})|. \quad (8)$$

Since we explicitly assume that the noise term in Equation (2) is entirely independent with \mathbf{z}_{t-1} , we enforce the independence of the estimated noise $\hat{\epsilon}_t^z$ and we have:

$$\ln p(\hat{\mathbf{z}}_t | \hat{\mathbf{z}}_{t-1}) = \ln p(\hat{\epsilon}_t^z) + \sum_{i=1}^n \ln \left| \frac{\partial r_i^A}{\partial \hat{\mathbf{z}}_{t-1,i}} \right|. \quad (9)$$

Therefore, the latent state prior can be estimated as follows:

$$\ln p(\hat{\mathbf{z}}_{1:T}) = \ln p(\hat{\mathbf{z}}_1) + \sum_{\tau=2}^t \left(\sum_{i=1}^n \ln p(\hat{\epsilon}_{\tau,i}^z) + \sum_{i=1}^n \ln \left| \frac{\partial r_i^A}{\partial \hat{\mathbf{z}}_{\tau-1,i}} \right| \right), \quad (10)$$

where $p(\hat{\epsilon}_i^z)$ follow Gaussian distributions. And another prior $p(\hat{\mathbf{z}}_{t+1:T} | \hat{\mathbf{z}}_{1:T})$ follows a similar derivation.

As for the missing cause prior estimator, we methodically employ a similar derivation. Then, we specifically designate $\{s_i^A\}$ as a set of learned inverse transition functions, which take the observed variables x_t^o and the missing cause $\hat{\mathbf{c}}_t$ as input, and output the noise term, i.e. $\hat{\epsilon}_t^c = s_i^A(x_t^o, \hat{\mathbf{c}}_{t,i})$.

Leaving s_i^A be an MLP, we further devise another transformation $\psi_c^A := \{x_t^o, \hat{\mathbf{c}}_t\} \rightarrow \{x_t^o, \hat{\epsilon}_t^c\}$ with its Jacobian is $\mathbf{J}_{\psi_c^A} = \begin{pmatrix} \mathbb{I} & 0 \\ * & \text{diag}\left(\frac{\partial s_i^A}{\partial \hat{\mathbf{c}}_{t,i}}\right) \end{pmatrix}$, where $*$ denotes a matrix. Similar to the derivation of latent state prior, we have:

$$\ln p(\hat{\mathbf{c}}_t | x_t^o) = \ln p(\hat{\epsilon}_t^c) + \sum_{i=1}^{n_c} \ln \left| \frac{\partial s_i^A}{\partial \hat{\mathbf{c}}_{t,i}} \right|. \quad (11)$$

Therefore, the missing cause prior can be estimated by maximizing the following equation, obtained by summing Equation (11) across time steps from 1 to t .

$$\ln p(\hat{\mathbf{c}}_{1:T} | x_{1:T}^o) = \sum_{\tau=1}^t \left(\sum_{i=1}^{n_c} \ln p(\hat{\epsilon}_{\tau,i}^c) + \sum_{i=1}^{n_c} \ln \left| \frac{\partial s_i^A}{\partial \hat{\mathbf{c}}_{\tau,i}} \right| \right). \quad (12)$$

3.3 DMM-MNAR model

To effectively address the time series imputation model under the MNAR mechanism, we devise the DMM-MNAR model, which is clearly shown in Figure 2(b).

Sequential Variational Backbone architecture for DMM-MNAR Similar to the DMM-MAR model, we employ the variational inference to model the data generation process of the MNAR mechanism, and the ELBO is

$$\begin{aligned} ELBO_B = & \underbrace{\mathbb{E}_{q(\mathbf{z}_{1:T}, \mathbf{c}_{1:T} | \mathbf{x}_{1:T})} \ln p(\mathbf{x}_{1:T}^m | \mathbf{z}_{1:T}, \mathbf{c}_{1:T})}_{\mathcal{L}_R} \\ & - \underbrace{D_{KL}(q(\mathbf{z}_{1:T} | \mathbf{x}_{1:T}^o) || p(\mathbf{z}_{1:T}))}_{\mathcal{L}_K^z} \\ & - \underbrace{D_{KL}(q(\mathbf{c}_{1:T} | \mathbf{x}_{1:T-1}) || p(\mathbf{c}_{1:T}))}_{\mathcal{L}_K^c}, \end{aligned} \quad (13)$$

¹We use the superscript symbol to denote estimated variables

Dataset	Ratio	DMM-MAR		DMM-MNAR		TimeCIB		ImputeFormer		TimesNet		SAITS		GPVAE		CSDI		BRITS		SSGAN	
		MSE	MAE	MSE	MAE	MSE	MAE	MSE	MAE	MSE	MAE	MSE	MAE	MSE	MAE	MSE	MAE	MSE	MAE	MSE	MAE
ETTh1	0.2	0.099	0.212	0.118	0.232	0.285	0.405	0.666	0.510	0.139	0.241	0.252	0.312	0.213	0.339	0.334	0.327	0.115	0.239	0.152	0.279
	0.4	0.165	0.259	0.184	0.297	0.389	0.471	0.705	0.579	0.207	0.294	0.185	0.286	0.280	0.407	0.523	0.438	0.175	0.277	0.172	0.280
	0.6	0.217	0.302	0.440	0.436	0.497	0.519	0.766	0.608	0.374	0.419	0.401	0.420	0.585	0.572	0.732	0.554	0.265	0.368	0.256	0.345
ETTh2	0.2	0.113	0.228	0.153	0.270	0.471	0.319	0.343	0.420	0.150	0.242	0.143	0.277	0.411	0.487	0.306	0.350	0.329	0.415	0.371	0.470
	0.4	0.214	0.339	0.233	0.347	0.543	0.487	0.542	0.551	0.386	0.434	0.672	0.591	0.463	0.521	0.567	0.484	0.444	0.486	0.747	0.692
	0.6	0.204	0.313	0.206	0.317	0.767	0.601	0.548	0.558	0.260	0.322	0.313	0.409	0.660	0.634	1.100	0.688	0.695	0.641	1.547	0.965
ETTm1	0.2	0.029	0.112	0.040	0.136	0.067	0.189	0.573	0.477	0.080	0.178	0.030	0.114	0.077	0.198	0.038	0.119	0.038	0.126	0.059	0.169
	0.4	0.039	0.129	0.061	0.165	0.099	0.229	0.585	0.488	0.127	0.221	0.041	0.134	0.109	0.237	0.049	0.132	0.046	0.137	0.078	0.198
	0.6	0.060	0.163	0.084	0.202	0.183	0.324	0.574	0.496	0.211	0.282	0.062	0.163	0.166	0.293	0.077	0.171	0.062	0.163	0.078	0.191
ETTm2	0.2	0.041	0.130	0.042	0.135	0.338	0.447	0.130	0.267	0.063	0.162	0.060	0.171	0.400	0.465	0.061	0.105	0.126	0.248	0.221	0.374
	0.4	0.044	0.138	0.055	0.155	0.444	0.506	0.177	0.303	0.085	0.187	0.070	0.184	0.401	0.479	0.141	0.149	0.166	0.288	0.129	0.261
	0.6	0.053	0.157	0.075	0.184	0.715	0.626	0.161	0.290	0.128	0.228	0.108	0.229	0.481	0.516	0.335	0.242	0.298	0.395	0.211	0.336
Exchange	0.2	0.003	0.038	0.009	0.051	0.314	0.281	0.178	0.283	0.013	0.063	0.085	0.231	0.711	0.712	0.017	0.076	0.319	0.493	0.666	0.711
	0.4	0.007	0.049	0.023	0.106	0.388	0.326	0.158	0.273	0.017	0.081	0.193	0.350	0.783	0.751	0.018	0.078	0.431	0.580	0.820	0.773
	0.6	0.008	0.058	0.030	0.121	0.445	0.372	0.201	0.296	0.024	0.101	0.224	0.382	0.834	0.771	0.055	0.143	0.669	0.707	1.235	0.961
Weather	0.2	0.029	0.050	0.049	0.084	0.049	0.113	0.099	0.153	0.038	0.077	0.040	0.078	0.055	0.128	0.069	0.057	0.034	0.059	0.035	0.077
	0.4	0.035	0.059	0.061	0.104	0.062	0.128	0.110	0.165	0.050	0.103	0.047	0.085	0.073	0.141	0.075	0.061	0.047	0.069	0.042	0.089
	0.6	0.040	0.070	0.080	0.132	0.082	0.152	0.110	0.167	0.061	0.119	0.058	0.090	0.082	0.160	0.074	0.053	0.072	0.058	0.053	0.111

Table 1: Experiment results in unsupervised scenarios for various datasets with different missing ratios under MAR conditions.

where D_{KL} denotes the KL divergence. Similar to DMM-MNAR, we let $q(\mathbf{z}_{1:T}|\mathbf{x}_{1:T}^o)$ and $q(\mathbf{c}_{1:T}|\mathbf{x}_{1:T-1})$ denote the encoders for the latent states \mathbf{z}_t and missing cause variables \mathbf{c}_t . They are formalized as follows:

$$\hat{\mathbf{z}}_{1:T} = \phi_{\mathbf{z}}^B(\mathbf{x}_{1:T}^o), \quad \hat{\mathbf{c}}_{1:T} = \phi_{\mathbf{c}}^B(\mathbf{x}_{1:T-1}), \quad (14)$$

Moreover, $p(\mathbf{x}_{1:T}|\mathbf{z}_{1:T}, \mathbf{c}_{1:T})$ denote the decoder for missing value prediction, which is formalized as follows:

$$\hat{\mathbf{x}}_{1:T}^m = F_B(\hat{\mathbf{z}}_{1:T}, \hat{\mathbf{c}}_{1:T}), \quad (15)$$

where F_B denotes the predictor and it is implemented by Multi-layer Perceptron networks (MLPs).

3.4 Prior Estimator for Temporal Latent States and Missing Cause Variables

Similarly, we also propose the latent state prior estimator and missing cause prior estimator to model the prior distributions of temporal latent states and missing cause variables.

As for the latent state prior estimator, we first let $\{r_i^B\}$ be a set of learned inverse transition functions that take the estimated latent variables and output the noise term, i.e., $\hat{\varepsilon}_{t,i}^z = r_i^B(\hat{\mathbf{z}}_{t,i}, \hat{\mathbf{z}}_{t-1})$ ² and each r_i^B is modeled with MLPs. Then we devise a transformation $\psi_z^B := \{\hat{\mathbf{z}}_{t-1}, \hat{\mathbf{z}}_t\} \rightarrow \{\hat{\mathbf{z}}_{t-1}, \hat{\varepsilon}_t^z\}$, and its Jacobian is $\mathbf{J}_{\psi_z^B} = \begin{pmatrix} \mathbb{I} & 0 \\ * & \text{diag}\left(\frac{\partial r_i^B}{\partial \hat{\mathbf{z}}_{t-1,i}}\right) \end{pmatrix}$, where $*$ denotes a matrix. By applying the change of variables formula, we have the following equation:

$$\ln p(\hat{\mathbf{z}}_{t-1}, \hat{\mathbf{z}}_t) = \ln p(\hat{\varepsilon}_t^z) + \ln |\det(\mathbf{J}_{\psi_z^B})|. \quad (16)$$

Since we explicitly assume that the noise term in Equation (2) is entirely independent with \mathbf{z}_{t-1} , we enforce the independence of the estimated noise $\hat{\varepsilon}_t^z$ and we have:

$$\ln p(\hat{\mathbf{z}}_t|\mathbf{z}_{t-1}) = \ln p(\hat{\varepsilon}_t^z) + \sum_{i=1}^n \ln \left| \frac{\partial r_i^B}{\partial \hat{\mathbf{z}}_{t-1,i}} \right|. \quad (17)$$

Therefore, the latent state prior can be estimated as follows:

$$\ln p(\hat{\mathbf{z}}_{1:t}) = \ln p(\hat{\mathbf{z}}_1) + \sum_{\tau=2}^t \left(\sum_{i=1}^n \ln p(\hat{\varepsilon}_{\tau,i}^z) + \sum_{i=1}^n \ln \left| \frac{\partial r_i^B}{\partial \hat{\mathbf{z}}_{\tau-1,i}} \right| \right), \quad (18)$$

²We use the superscript symbol to denote estimated variables.

where $p(\hat{\varepsilon}_t^z)$ follow Gaussian distributions. And another prior $p(\hat{\mathbf{z}}_{t+1:T}|\hat{\mathbf{z}}_{1:t})$ follows a similar derivation.

As for the missing cause prior estimator, The prior distribution of missing cause can be formalized as: As for the missing cause prior estimator, we employ a similar derivation and let $\{s_i^B\}$ be a set of learned inverse transition functions, which take the time series data x_{t-1} and missing cause $\hat{\mathbf{c}}_t$ as input and output the noise term, i.e. $\hat{\varepsilon}_t^c = s_i^B(\hat{\mathbf{x}}_{t-1}^o, \hat{\mathbf{x}}_{t-1}^m, \hat{\mathbf{c}}_{t,i})$.

Leaving s_i^B be an MLP, we further devise another transformation $\psi_c^B := \{\mathbf{x}_{t-1}^o, \hat{\mathbf{x}}_{t-1}^m, \hat{\mathbf{c}}_t\} \rightarrow \{\mathbf{x}_{t-1}^o, \hat{\mathbf{x}}_{t-1}^m, \hat{\varepsilon}_t^c\}$ with its Jacobian is $\mathbf{J}_{\psi_c^B} = \begin{pmatrix} \mathbb{I} & 0 \\ * & \text{diag}\left(\frac{\partial s_i^B}{\partial \hat{\mathbf{c}}_{t,i}}\right) \end{pmatrix}$, where $*$ denotes a matrix. Similar to latent state prior derivation, we have:

$$\ln p(\hat{\mathbf{c}}_t|x_{t-1}^o, \hat{\mathbf{x}}_{t-1}^m) = \ln p(\hat{\varepsilon}_t^c) + \sum_{i=1}^{n_c} \ln \left| \frac{\partial s_i^B}{\partial \hat{\mathbf{c}}_{t,i}} \right|. \quad (19)$$

Therefore, the missing cause prior can be estimated by maximizing the following equation, obtained by summing Equation (19) across time steps from 1 to t.

$$\begin{aligned} \ln p(\hat{\mathbf{c}}_{1:t}|x_{1:t-1}^o, \hat{\mathbf{x}}_{1:t-1}^m) &= \ln p(\hat{\mathbf{c}}_1) \\ &+ \sum_{\tau=2}^t \left(\sum_{i=1}^{n_c} \ln p(\hat{\varepsilon}_{\tau,i}^c) + \sum_{i=1}^{n_c} \ln \left| \frac{\partial s_i^B}{\partial \hat{\mathbf{c}}_{\tau,i}} \right| \right). \end{aligned} \quad (20)$$

3.5 Model Summary

The difference between the DMM-MAR and DMM-MNAR is the prior estimator. For DMM-MAR, we use the \mathbf{x}_t^o to estimate the prior distribution of \mathbf{c}_t . For DMM-MNAR, we use the \mathbf{x}_{t-1}^o and \mathbf{x}_{t-1}^m to estimate the prior distribution of \mathbf{c}_t .

By estimating the prior distribution of latent states and missing causes, we can calculate the KL divergence in Equations (5) and (13). So we can optimize the ELBO to model the data generation processes. The total loss of the proposed two models can be formalized as follows:

$$\mathcal{L}_{total} = \mathcal{L}_R + \beta \mathcal{L}_K^z + \gamma \mathcal{L}_K^c, \quad (21)$$

where β and γ are hyperparameters.

In real-world scenarios full of complexity, we do not know which type of missing data mechanism applies. However, we can use model selection methods by running two models on the same data and choosing the one that yields better results. We will verify this in the experimental section.

Dataset	Ratio	DMM-MAR		DMM-MNAR		TimeCIB		ImputeFormer		TimesNet		SAITS		GPVAE		CSDI		BRITS		SSGAN	
		MSE	MAE	MSE	MAE	MSE	MAE	MSE	MAE	MSE	MAE	MSE	MAE	MSE	MAE	MSE	MAE	MSE	MAE	MSE	MAE
ETTh1	0.2	0.138	0.240	0.108	0.230	0.327	0.475	0.651	0.503	0.149	0.248	0.165	0.271	0.256	0.375	0.326	0.324	0.125	0.248	0.149	0.281
	0.4	0.238	0.329	0.171	0.280	0.392	0.492	0.691	0.530	0.220	0.306	0.265	0.330	0.362	0.442	0.497	0.424	0.177	0.294	0.172	0.301
	0.6	0.323	0.384	0.262	0.358	0.484	0.517	0.689	0.538	0.309	0.373	0.308	0.363	0.405	0.467	0.659	0.521	0.297	0.388	0.271	0.377
ETTh2	0.2	0.088	0.197	0.078	0.187	0.501	0.416	0.172	0.348	0.127	0.230	0.143	0.273	0.389	0.486	0.229	0.309	0.211	0.334	0.306	0.421
	0.4	0.099	0.216	0.089	0.200	0.563	0.482	0.299	0.387	0.187	0.273	0.218	0.340	0.572	0.573	0.516	0.472	0.293	0.402	0.653	0.644
	0.6	0.178	0.268	0.133	0.255	0.647	0.569	0.450	0.471	0.325	0.353	0.293	0.396	0.831	0.704	0.946	0.646	0.547	0.580	0.334	0.423
ETTm1	0.2	0.038	0.131	0.025	0.104	0.079	0.206	0.608	0.481	0.082	0.179	0.028	0.110	0.080	0.204	0.032	0.110	0.031	0.113	0.059	0.166
	0.4	0.053	0.157	0.039	0.133	0.104	0.242	0.576	0.480	0.128	0.222	0.042	0.133	0.104	0.230	0.049	0.134	0.041	0.139	0.074	0.192
	0.6	0.075	0.192	0.061	0.168	0.146	0.289	0.591	0.501	0.208	0.281	0.066	0.171	0.156	0.287	0.088	0.179	0.073	0.179	0.070	0.182
ETTm2	0.2	0.047	0.135	0.045	0.134	0.439	0.497	0.124	0.251	0.059	0.157	0.046	0.143	0.226	0.351	0.059	0.189	0.127	0.254	0.164	0.310
	0.4	0.052	0.148	0.049	0.146	0.569	0.579	0.151	0.274	0.115	0.213	0.076	0.194	0.413	0.489	0.061	0.194	0.159	0.277	0.085	0.193
	0.6	0.072	0.174	0.066	0.174	0.647	0.782	0.142	0.271	0.158	0.243	0.090	0.206	0.500	0.523	0.096	0.254	0.221	0.324	0.159	0.280
Exchange	0.2	0.007	0.052	0.004	0.044	0.526	0.471	0.150	0.262	0.014	0.070	0.117	0.274	0.749	0.741	0.016	0.076	0.461	0.574	0.586	0.651
	0.4	0.007	0.060	0.006	0.053	0.552	0.479	0.201	0.298	0.016	0.079	0.191	0.342	0.790	0.760	0.015	0.077	0.565	0.637	0.756	0.729
	0.6	0.009	0.063	0.008	0.061	0.574	0.487	0.488	0.578	0.024	0.099	0.212	0.370	0.808	0.765	0.041	0.135	0.747	0.750	0.811	0.765
Weather	0.2	0.054	0.087	0.032	0.052	0.045	0.094	0.105	0.148	0.041	0.077	0.041	0.071	0.055	0.116	0.059	0.065	0.037	0.056	0.035	0.073
	0.4	0.041	0.069	0.038	0.062	0.061	0.126	0.104	0.157	0.054	0.093	0.050	0.076	0.075	0.147	0.073	0.080	0.057	0.067	0.042	0.090
	0.6	0.071	0.119	0.043	0.075	0.074	0.139	0.113	0.160	0.066	0.117	0.057	0.093	0.091	0.166	0.082	0.093	0.070	0.079	0.048	0.093

Table 2: Experiment results in unsupervised scenarios for various datasets with different missing ratios under MNAR conditions.

4 Identification Results

In this section, we aim to show that the identifiability for latent state \mathbf{z}_t and missing causes \mathbf{c}_t under the MAR and MNAR missing mechanisms, providing a theoretical guarantee for the DMM framework. Specifically, we say \mathbf{z}_t is ‘identifiable’ if, for each ground-truth changing latent variables \mathbf{z}_t , there exists a corresponding estimated component $\hat{\mathbf{z}}_t$ and an invertible function $h^z : \mathbb{R}^n \rightarrow \mathbb{R}^n$, such that $\mathbf{z}_t = h^z(\hat{\mathbf{z}}_t)$. The same applies to \mathbf{c}_t . Next, we first show how the \mathbf{z}_t and \mathbf{c}_t are identifiable under MAR.

Theorem 1. (Identification of Latent States and Missing Causes under MAR.) Suppose that the observed data from missing time series data is generated following the data generation process, and we make the following assumptions:

- A1 (Smooth, Positive and Conditional independent Density:)** [Yao et al., 2022; Yao et al., 2021] The probability density function of latent variables is smooth and positive, i.e., $p(\mathbf{z}_t|\mathbf{z}_{t-1}) > 0$, $p(\mathbf{c}_t|\mathbf{x}_t^o) > 0$. Conditioned on \mathbf{z}_{t-1} each $\mathbf{z}_{t,i}$ is independent of any other $\mathbf{z}_{t,j}$ for $i, j \in 1, \dots, n, i \neq j$, i.e., $\log p(\mathbf{z}_t|\mathbf{z}_{t-1}) = \sum_{k=1}^{n_s} \log p(\mathbf{z}_{t,k}|\mathbf{z}_{t-1})$. Conditioned on \mathbf{x}^o each $\mathbf{c}_{t,i}$ is independent of any other $\mathbf{c}_{t,j}$ for $i, j \in 1, \dots, n, i \neq j$, i.e., $\log p(\mathbf{c}_t|\mathbf{x}_t^o) = \sum_{k=1}^{n_s} \log p(\mathbf{c}_{t,k}|\mathbf{x}_t^o)$.
- A2 (Linear Independent of MAR:)** [Yao et al., 2022] For any \mathbf{z}_t , there exist $2n+1$ values of $z_{t-1,l}, l = 1, \dots, n$, such that these $2n$ vectors $\mathbf{v}_{t,k,l}^B - \mathbf{v}_{t,k,n}^B$ are linearly independent, where $\mathbf{v}_{t,k,l}^B$ is defined as follows:

$$\mathbf{v}_{t,k,l}^B = \left(\frac{\partial^2 \log p(z_{t,k}|\mathbf{z}_{t-1})}{\partial z_{t,k} \partial z_{t-1,1}}, \dots, \frac{\partial^2 \log p(z_{t,k}|\mathbf{z}_{t-1})}{\partial z_{t,k} \partial z_{t-1,n}}, \frac{\partial^3 \log p(z_{t,k}|\mathbf{z}_{t-1})}{\partial^2 z_{t,k} \partial z_{t-1,1}}, \dots, \frac{\partial^3 \log p(z_{t,k}|\mathbf{z}_{t-1})}{\partial^2 z_{t,k} \partial z_{t-1,n}} \right)^T$$

Similarly, for each value of \mathbf{c}_t , there exist $2n+1$ values of \mathbf{x}_{t-1}^o , i.e., $\mathbf{x}_{t-1,j}^o$ with $j = 0, 2, \dots, 2n$, such that these $2n$ vectors $\mathbf{w}^A(\mathbf{c}_t, \mathbf{x}_{t-1,j}^o) - \mathbf{w}^A(\mathbf{c}_t, \mathbf{x}_{t-1,0}^o)$ are linearly independent, where the vector $\mathbf{w}^A(\mathbf{c}_t, \mathbf{x}_{t-1,j}^o)$ is defined as follows:

$$\mathbf{w}^A(\mathbf{c}_t, \mathbf{x}_{t-1,j}^o) = \left(\frac{\partial^2 \log p(c_{t,k}|\mathbf{x}_t^o)}{\partial^2 c_{t,k}}, \dots, \frac{\partial^2 \log p(c_{t,k}|\mathbf{x}_t^o)}{\partial^2 c_{t,k}}, \frac{\partial \log p(c_{t,k}|\mathbf{x}_t^o)}{\partial c_{t,k}}, \dots, \frac{\partial \log p(c_{t,k}|\mathbf{x}_t^o)}{\partial c_{t,k}} \right)^T$$

Then, by learning the data generation process, \mathbf{z}_t and \mathbf{c}_t are component-wise identifiable.

Generally speaking, the linear independent condition is quite common in [Kong et al., 2022; Li et al., 2024a; Yao et al., 2022], implying that the sufficient changes are mainly led by the auxiliary valuable such as the historical information \mathbf{z}_{t-1} and the observed variables \mathbf{x}_t^o .

Theorem 2. (Identification of Latent States and Missing Causes under MNAR.) We follow the A1 in Theorem 1 and suppose that the observed data from missing time series data is generated following the data generation process, and we further make the following assumptions:

- A3 (Linear Independence of MNAR:)** [Yao et al., 2022] For any \mathbf{z}_t , there exist $2n+1$ values of $z_{t-1,l}, l = 1, \dots, n$, such that these $2n$ vectors $\mathbf{v}_{t,k,l}^B - \mathbf{v}_{t,k,n}^B$ are linearly independent, where $\mathbf{v}_{t,k,l}^B$ is defined as follows:

$$\mathbf{v}_{t,k,l}^B = \left(\frac{\partial^2 \log p(z_{t,k}|\mathbf{z}_{t-1})}{\partial z_{t,k} \partial z_{t-1,1}}, \dots, \frac{\partial^2 \log p(z_{t,k}|\mathbf{z}_{t-1})}{\partial z_{t,k} \partial z_{t-1,n}}, \frac{\partial^3 \log p(z_{t,k}|\mathbf{z}_{t-1})}{\partial^2 z_{t,k} \partial z_{t-1,1}}, \dots, \frac{\partial^3 \log p(z_{t,k}|\mathbf{z}_{t-1})}{\partial^2 z_{t,k} \partial z_{t-1,n}} \right)^T$$

Similarly, for each value of \mathbf{c}_t , there exist $2n+1$ values of \mathbf{x}_{t-1}^o , i.e., $\mathbf{x}_{t-1,j}^o$ with $j = 0, 2, \dots, 2n$, such that these $2n$ vectors $\mathbf{w}^B(\mathbf{c}_t, \mathbf{x}_{t-1,j}^o) - \mathbf{w}^B(\mathbf{c}_t, \mathbf{x}_{t-1,0}^o)$ are linearly independent, where $\mathbf{w}^B(\mathbf{c}_t, \mathbf{x}_{t-1,j}^o)$ is defined as follows:

$$\begin{aligned} \mathbf{w}^B(\mathbf{c}_t, \mathbf{x}_{t-1,j}^o) &= \left(\frac{\partial^2 \log p(c_{t,k}|\mathbf{x}_{t-1}^o)}{\partial^2 c_{t,k}}, \dots, \frac{\partial^2 \log p(c_{t,k}|\mathbf{x}_{t-1}^o)}{\partial^2 c_{t,k}}, \frac{\partial \log p(c_{t,k}|\mathbf{x}_{t-1}^o)}{\partial c_{t,k}}, \dots, \frac{\partial \log p(c_{t,k}|\mathbf{x}_{t-1}^o)}{\partial c_{t,k}} \right)^T \end{aligned} \quad (22)$$

Then, by learning the data generation process, \mathbf{z}_t and \mathbf{c}_t are component-wise identifiable.

Similar to Theorem 1, the linear independence assumptions are also standard in existing works of identification. The proof can be found in Appendix C. Please refer to Appendix E, G for explanation of these assumptions of our theoretical results, limitation as well as the potential solution.

Dataset	A-MAR			A-MNAR		
Ratio	0.2	0.4	0.6	0.2	0.4	0.6
DMM-MAR	0.92	0.91	0.908	0.894	0.87	0.868
DMM-MNAR	0.905	0.887	0.872	0.933	0.917	0.872

Table 3: Experiments results of MCC on simulation data.

5 Experiments

5.1 Experiments on Simulation Data

Dataset. We generated simulated time series data A using Equations (1)-(2) and the fixed latent causal processes given in Figure 1 (b)(c), which have three latent variables. We generated corresponding mask matrices based on two different missing mechanisms, MAR and MNAR, to simulate missing values. In addition, to investigate the impact of missing ratios on the results, we specifically set three different missing ratios of 0.2, 0.4, and 0.6. Please refer to Appendix B for the details of data generation and evaluation metrics.

Experiment Results. The experimental results of the simulated dataset are shown in Table 3. With the experimental results, we can draw the following conclusions: 1) We observe that our model has high estimation accuracy in both datasets with different missing mechanisms. 2) As the missing rate increases, the MCC score will also decrease. The lack of data has a significant impact on the identifiability performance of the model. 3) We also find that models considering the corresponding missing mechanism have higher MCC scores on the dataset under this missing mechanism. Under the MAR missing mechanism, the MCC score of the DMM-MAR model is higher than that of the DMM-MNAR model. This indicates that when the missing data mechanism is unknown, the corresponding model can effectively improve performance. Please refer to Appendix B for experimental results of MCC on missing cause variable **c** and sensitivity analysis.

5.2 Experiments on Real-World Data

Dataset. To evaluate the performance of the proposed method, we consider the following datasets: 1) **ETT**[Zhou *et al.*, 2021]: {ETTh1, ETTh2, ETTm1, ETTm2}; 2) **Exchange**[Lai *et al.*, 2018]; 3) **Weather**³; For each dataset, we systematically generate mask matrices to accurately simulate missing values based on the missing mechanisms of MAR and MNAR. Meanwhile, we use three different mask ratios, such as 0.2, 0.4, and 0.6. In addition, we use both supervised learning and unsupervised learning methods for training. Please refer to Appendix B for a detailed introduction to the dataset and information on data preprocessing.

Baselines. In order to assess the efficacy of our proposed Deep Missingness Model (DMM), we juxtaposed it against an array of cutting-edge deep learning models designed for time series data imputation. We initially turned our attention towards models that employ the Attention mechanism, including SAITS [Du *et al.*, 2023], and ImputeFormer [Nie *et al.*, 2023]. Subsequently, we broadened our scope to include the Diffusion Model-based method as CSDI [Tashiro *et al.*,

³<https://www.bgc-jena.mpg.de/wetter/>

2021], and TimesNet [Wu *et al.*, 2022], which utilizes Convolutional Neural Networks (CNN). Furthermore, we took into account BRITS [Cao *et al.*, 2018] which is based on RNN, and SSGAN [Miao *et al.*, 2021] which is founded on GAN. In the final stage of our comparison, we considered TimeCIB [Choi and Lee, 2023] and GPVAE [Fortuin *et al.*, 2020], both of which are based on the Variational Autoencoder (VAE) architecture. In a bid to underline the significance of accounting for data loss mechanisms, we applied our model variants to two distinct datasets that were subjected to different data loss treatments. We then compared their performances under identical parameter settings. To ensure the robustness of our findings, each experiment was repeated thrice using random seeds, and the mean performance was subsequently reported.

Experiment Results. The results of our unsupervised learning experiments are tabulated in Tables 1 and Table 2. For each experimental configuration, we conducted three independent trials with varying random seeds and reported the mean and standard deviation of the results. Please refer to Appendix B for the results of supervised learning experiments and the standard deviation of experimental results. We can draw the following conclusions: 1) Our model exhibits a superior performance ranging from 0.5% to 52% compared to the most competitive baseline, while also considerably diminishing the imputation error in the Exchange dataset. 2) Compared to existing methods that do not consider different missing mechanisms, our DMM model demonstrates significantly better performance when a correct missing mechanism is used. 3) Since some comparison methods like TimeCIB and ImputeFormer only consider a single missing mechanism, they tend to suffer from mismatched mechanisms and result in degenerated performance. Meanwhile, our DMM model outshines all other baselines across the majority of imputation tasks when the missing mechanism is used correctly. 4) Moreover, when our method is applied to a mismatched missing data mechanism, for instance, using DMM-MAR on MNAR datasets—the performance is inferior to that of the correctly matched model. This demonstrates that model selection can be effectively used when the missing data mechanism is unknown. Please refer to Appendix B for experimental results on the MIMIC healthcare dataset, future time-step influence, mixed missing mechanisms, ablation studies, and computational efficiency analysis.

6 Conclusion

We introduce a causal perspective on the time series imputation problem, formalizing different mechanisms of data missingness within an imputation m-graph. Based on this, we propose a novel framework called Different Missing Mechanisms (DMM), which effectively addresses the mechanism mismatching problem inherent in existing methods. The DMM framework adeptly handles both MAR and MNAR missing mechanisms by incorporating the relevant data generation processes, while also ensuring identifiability. Extensive experiments on several benchmark datasets demonstrate the effectiveness of our approach. Our theoretical results and the proposed framework represent a significant advancement in time series imputation and causal representation learning.

Acknowledgments

This research was supported in part by National Science and Technology Major Project (2021ZD0111501), National Science Fund for Excellent Young Scholars (62122022), Natural Science Foundation of China (U24A20233, 62476163, 62406078), Guangdong Basic and Applied Basic Research Foundation (2023B1515120020).

References

[Acuna and Rodriguez, 2004] Edgar Acuna and Caroline Rodriguez. The treatment of missing values and its effect on classifier accuracy. In *Classification, Clustering, and Data Mining Applications: Proceedings of the Meeting of the International Federation of Classification Societies (IFCS), Illinois Institute of Technology, Chicago, 15–18 July 2004*, pages 639–647. Springer, 2004.

[Alcaraz and Strodtthoff, 2022] Juan Miguel Lopez Alcaraz and Nils Strodtthoff. Diffusion-based time series imputation and forecasting with structured state space models. *arXiv preprint arXiv:2208.09399*, 2022.

[Allman *et al.*, 2009] Elizabeth S Allman, Catherine Matias, and John A Rhodes. Identifiability of parameters in latent structure models with many observed variables. 2009.

[Cai *et al.*, 2025a] Ruichu Cai, Haiqin Huang, Zhifan Jiang, Zijian Li, Changze Zhou, Yuequn Liu, Yuming Liu, and Zhifeng Hao. Disentangling long-short term state under unknown interventions for online time series forecasting. In *Proceedings of the AAAI Conference on Artificial Intelligence*, volume 39, pages 15641–15649, 2025.

[Cai *et al.*, 2025b] Ruichu Cai, Zhifan Jiang, Kaitao Zheng, Zijian Li, Weilin Chen, Xuexin Chen, Yifan Shen, Guangyi Chen, Zhifeng Hao, and Kun Zhang. Learning disentangled representation for multi-modal time-series sensing signals. In *Proceedings of the ACM on Web Conference 2025*, pages 3247–3266, 2025.

[Cai *et al.*, 2025c] Ruichu Cai, Junjie Wan, Weilin Chen, Ze-qin Yang, Zijian Li, Peng Zhen, and Jiecheng Guo. Long-term individual causal effect estimation via identifiable latent representation learning. 2025.

[Cao *et al.*, 2018] Wei Cao, Dong Wang, Jian Li, Hao Zhou, Lei Li, and Yitan Li. Brits: Bidirectional recurrent imputation for time series. *Advances in neural information processing systems*, 31, 2018.

[Che *et al.*, 2018] Zhengping Che, Sanjay Purushotham, Kyunghyun Cho, David Sontag, and Yan Liu. Recurrent neural networks for multivariate time series with missing values. *Scientific reports*, 8(1):6085, 2018.

[Chen *et al.*, 2023] Yu Chen, Wei Deng, Shikai Fang, Feng-pei Li, Nicole Tianjiao Yang, Yikai Zhang, Kashif Rasul, Shandian Zhe, Anderson Schneider, and Yuriy Nevmyvaka. Provably convergent schrödinger bridge with applications to probabilistic time series imputation. In *International Conference on Machine Learning*, pages 4485–4513. PMLR, 2023.

[Chen *et al.*, 2024] Guangyi Chen, Yifan Shen, Zhenhao Chen, Xiangchen Song, Yuwen Sun, Weiran Yao, Xiaoliu, and Kun Zhang. Caring: Learning temporal causal representation under non-invertible generation process. *arXiv preprint arXiv:2401.14535*, 2024.

[Choi and Lee, 2023] MinGyu Choi and Changhee Lee. Conditional information bottleneck approach for time series imputation. In *The Twelfth International Conference on Learning Representations*, 2023.

[Cini *et al.*, 2021] Andrea Cini, Ivan Marisca, and Cesare Alippi. Filling the $g_{\text{ap_s}}$: Multivariate time series imputation by graph neural networks. *arXiv preprint arXiv:2108.00298*, 2021.

[Comon, 1994] Pierre Comon. Independent component analysis, a new concept? *Signal processing*, 36(3):287–314, 1994.

[Daunhawer *et al.*, 2023] Imant Daunhawer, Alice Bizeul, Emanuele Palumbo, Alexander Marx, and Julia E Vogt. Identifiability results for multimodal contrastive learning. *arXiv preprint arXiv:2303.09166*, 2023.

[Dempster *et al.*, 1977] Arthur P Dempster, Nan M Laird, and Donald B Rubin. Maximum likelihood from incomplete data via the em algorithm. *Journal of the royal statistical society: series B (methodological)*, 39(1):1–22, 1977.

[Du *et al.*, 2023] Wenjie Du, David Côté, and Yan Liu. Saits: Self-attention-based imputation for time series. *Expert Systems with Applications*, 219:119619, 2023.

[Fang *et al.*, 2023] Shikai Fang, Qingsong Wen, Shandian Zhe, and Liang Sun. Bayotide: Bayesian online multivariate time series imputation with functional decomposition. *arXiv preprint arXiv:2308.14906*, 2023.

[Fortuin *et al.*, 2020] Vincent Fortuin, Dmitry Baranchuk, Gunnar Rätsch, and Stephan Mandt. Gp-vae: Deep probabilistic time series imputation. In *International conference on artificial intelligence and statistics*, pages 1651–1661. PMLR, 2020.

[Gibb *et al.*, 2006] Brandon E Gibb, Christopher G Beevers, Margaret S Andover, and Kyle Holleran. The hopelessness theory of depression: A prospective multi-wave test of the vulnerability-stress hypothesis. *Cognitive Therapy and Research*, 30:763–772, 2006.

[Grella *et al.*, 2008] Christine E Grella, Christy K Scott, Mark A Foss, and Michael L Dennis. Gender similarities and differences in the treatment, relapse, and recovery cycle. *Evaluation review*, 32(1):113–137, 2008.

[Gresele *et al.*, 2020] Luigi Gresele, Paul K Rubenstein, Arash Mehrjou, Francesco Locatello, and Bernhard Schölkopf. The incomplete rosetta stone problem: Identifiability results for multi-view nonlinear ica. In *Uncertainty in Artificial Intelligence*, pages 217–227. PMLR, 2020.

[Hälvä and Hyvärinen, 2020] Hermanni Hälvä and Aapo Hyvärinen. Hidden markov nonlinear ica: Unsupervised learning from nonstationary time series. In *Conference*

on *Uncertainty in Artificial Intelligence*, pages 939–948. PMLR, 2020.

[Huang *et al.*, 2023] Zenan Huang, Haobo Wang, Junbo Zhao, and Nenggan Zheng. Latent processes identification from multi-view time series. *arXiv preprint arXiv:2305.08164*, 2023.

[Hyvarinen and Morioka, 2016] Aapo Hyvarinen and Hiroshi Morioka. Unsupervised feature extraction by time-contrastive learning and nonlinear ica. *Advances in neural information processing systems*, 29, 2016.

[Hyvarinen and Morioka, 2017] Aapo Hyvarinen and Hiroshi Morioka. Nonlinear ica of temporally dependent stationary sources. In *Artificial Intelligence and Statistics*, pages 460–469. PMLR, 2017.

[Hyvärinen and Pajunen, 1999] Aapo Hyvärinen and Petteri Pajunen. Nonlinear independent component analysis: Existence and uniqueness results. *Neural networks*, 12(3):429–439, 1999.

[Hyvarinen *et al.*, 2019] Aapo Hyvarinen, Hiroaki Sasaki, and Richard Turner. Nonlinear ica using auxiliary variables and generalized contrastive learning. In *The 22nd International Conference on Artificial Intelligence and Statistics*, pages 859–868. PMLR, 2019.

[Hyvärinen *et al.*, 2024] Aapo Hyvärinen, Ilyes Khemakhem, and Ricardo Monti. Identifiability of latent-variable and structural-equation models: from linear to nonlinear. *Annals of the Institute of Statistical Mathematics*, 76(1):1–33, 2024.

[Hyvärinen, 2013] Aapo Hyvärinen. Independent component analysis: recent advances. *Philosophical Transactions of the Royal Society A: Mathematical, Physical and Engineering Sciences*, 371(1984):20110534, 2013.

[Jiang *et al.*, 2023] Jiawei Jiang, Chengkai Han, Wayne Xin Zhao, and Jingyuan Wang. Pdformer: Propagation delay-aware dynamic long-range transformer for traffic flow prediction. In *Proceedings of the AAAI conference on artificial intelligence*, volume 37, pages 4365–4373, 2023.

[Johnson *et al.*, 2016] Alistair EW Johnson, Tom J Pollard, Lu Shen, Li-wei H Lehman, Mengling Feng, Mohammad Ghassemi, Benjamin Moody, Peter Szolovits, Leo Anthony Celi, and Roger G Mark. Mimic-iii, a freely accessible critical care database. *Scientific data*, 3(1):1–9, 2016.

[Khemakhem *et al.*, 2020a] Ilyes Khemakhem, Diederik Kingma, Ricardo Monti, and Aapo Hyvarinen. Variational autoencoders and nonlinear ica: A unifying framework. In *International conference on artificial intelligence and statistics*, pages 2207–2217. PMLR, 2020.

[Khemakhem *et al.*, 2020b] Ilyes Khemakhem, Ricardo Monti, Diederik Kingma, and Aapo Hyvarinen. Ice-beem: Identifiable conditional energy-based deep models based on nonlinear ica. *Advances in Neural Information Processing Systems*, 33:12768–12778, 2020.

[Kim *et al.*, 2023] SeungHyun Kim, Hyunsu Kim, Eunggu Yun, Hwangrae Lee, Jaehun Lee, and Juho Lee. Probabilistic imputation for time-series classification with missing data. In *International Conference on Machine Learning*, pages 16654–16667. PMLR, 2023.

[Kong *et al.*, 2022] Lingjing Kong, Shaoan Xie, Weiran Yao, Yujia Zheng, Guangyi Chen, Petar Stojanov, Victor Akinwande, and Kun Zhang. Partial disentanglement for domain adaptation. In *International conference on machine learning*, pages 11455–11472. PMLR, 2022.

[Kong *et al.*, 2023] Lingjing Kong, Biwei Huang, Feng Xie, Eric Xing, Yuejie Chi, and Kun Zhang. Identification of nonlinear latent hierarchical models. *Advances in Neural Information Processing Systems*, 36:2010–2032, 2023.

[Lachapelle and Lacoste-Julien, 2022] Sébastien Lachapelle and Simon Lacoste-Julien. Partial disentanglement via mechanism sparsity. *arXiv preprint arXiv:2207.07732*, 2022.

[Lachapelle *et al.*, 2023] Sébastien Lachapelle, Tristan Deleu, Divyat Mahajan, Ioannis Mitliagkas, Yoshua Bengio, Simon Lacoste-Julien, and Quentin Bertrand. Synergies between disentanglement and sparsity: Generalization and identifiability in multi-task learning. In *International Conference on Machine Learning*, pages 18171–18206. PMLR, 2023.

[Lai *et al.*, 2018] Guokun Lai, Wei-Cheng Chang, Yiming Yang, and Hanxiao Liu. Modeling long-and short-term temporal patterns with deep neural networks. In *The 41st international ACM SIGIR conference on research & development in information retrieval*, pages 95–104, 2018.

[Lee and Lee, 1998] Te-Won Lee and Te-Won Lee. *Independent component analysis*. Springer, 1998.

[Li *et al.*, 2023] Zijian Li, Zunhong Xu, Ruichu Cai, Zhenhui Yang, Yuguang Yan, Zhifeng Hao, Guangyi Chen, and Kun Zhang. Identifying semantic component for robust molecular property prediction. *arXiv preprint arXiv:2311.04837*, 2023.

[Li *et al.*, 2024a] Zijian Li, Ruichu Cai, Guangyi Chen, Boyang Sun, Zhifeng Hao, and Kun Zhang. Subspace identification for multi-source domain adaptation. *Advances in Neural Information Processing Systems*, 36, 2024.

[Li *et al.*, 2024b] Zijian Li, Ruichu Cai, Zhenhui Yang, Haiqin Huang, Guangyi Chen, Yifan Shen, Zhengming Chen, Xiangchen Song, and Kun Zhang. When and how: Learning identifiable latent states for nonstationary time series forecasting. *arXiv preprint arXiv:2402.12767*, 2024.

[Li *et al.*, 2025] Zijian Li, Yifan Shen, Kaitao Zheng, Ruichu Cai, Xiangchen Song, Mingming Gong, Guangyi Chen, and Kun Zhang. On the identification of temporal causal representation with instantaneous dependence. In *The Thirteenth International Conference on Learning Representations*, 2025.

[Lippe *et al.*, 2022] Phillip Lippe, Sara Magliacane, Sindy Löwe, Yuki M Asano, Taco Cohen, and Stratis Gavves. Citris: Causal identifiability from temporal intervened sequences. In *International Conference on Machine Learning*, pages 13557–13603. PMLR, 2022.

[Liu *et al.*, 2019] Yukai Liu, Rose Yu, Stephan Zheng, Eric Zhan, and Yisong Yue. Naomi: Non-autoregressive multiresolution sequence imputation. *Advances in neural information processing systems*, 32, 2019.

[Liu *et al.*, 2023a] Mingzhe Liu, Han Huang, Hao Feng, Leilei Sun, Bowen Du, and Yanjie Fu. Pristi: A conditional diffusion framework for spatiotemporal imputation. In *2023 IEEE 39th International Conference on Data Engineering (ICDE)*, pages 1927–1939. IEEE, 2023.

[Liu *et al.*, 2023b] Yong Liu, Tengge Hu, Haoran Zhang, Haixu Wu, Shiyu Wang, Lintao Ma, and Mingsheng Long. itransformer: Inverted transformers are effective for time series forecasting. *arXiv preprint arXiv:2310.06625*, 2023.

[Liu *et al.*, 2023c] Yuejiang Liu, Alexandre Alahi, Chris Russell, Max Horn, Dominik Zietlow, Bernhard Schölkopf, and Francesco Locatello. Causal triplet: An open challenge for intervention-centric causal representation learning. In *Conference on Causal Learning and Reasoning*, pages 553–573. PMLR, 2023.

[Locatello *et al.*, 2019] Francesco Locatello, Stefan Bauer, Mario Lucic, Gunnar Raetsch, Sylvain Gelly, Bernhard Schölkopf, and Olivier Bachem. Challenging common assumptions in the unsupervised learning of disentangled representations. In *international conference on machine learning*, pages 4114–4124. PMLR, 2019.

[Luo *et al.*, 2018] Yonghong Luo, Xiangrui Cai, Ying Zhang, Jun Xu, et al. Multivariate time series imputation with generative adversarial networks. *Advances in neural information processing systems*, 31, 2018.

[Mansouri *et al.*, 2023] Amin Mansouri, Jason Hartford, Yan Zhang, and Yoshua Bengio. Object-centric architectures enable efficient causal representation learning. *arXiv preprint arXiv:2310.19054*, 2023.

[Marisca *et al.*, 2022] Ivan Marisca, Andrea Cini, and Cesare Alippi. Learning to reconstruct missing data from spatiotemporal graphs with sparse observations. *Advances in Neural Information Processing Systems*, 35:32069–32082, 2022.

[Miao *et al.*, 2021] Xiaoye Miao, Yangyang Wu, Jun Wang, Yunjun Gao, Xudong Mao, and Jianwei Yin. Generative semi-supervised learning for multivariate time series imputation. In *Proceedings of the AAAI conference on artificial intelligence*, volume 35, pages 8983–8991, 2021.

[Mohan *et al.*, 2013] Karthika Mohan, Judea Pearl, and Jin Tian. Graphical models for inference with missing data. *Advances in neural information processing systems*, 26, 2013.

[Mulyadi *et al.*, 2021] Ahmad Wisnu Mulyadi, Eunji Jun, and Heung-Il Suk. Uncertainty-aware variational recurrent imputation network for clinical time series. *IEEE Transactions on Cybernetics*, 52(9):9684–9694, 2021.

[Nie *et al.*, 2023] Tong Nie, Guoyang Qin, Wei Ma, Yuewen Mei, and Jian Sun. Imputeformer: Low rankness-induced transformers for generalizable spatiotemporal imputation. *arXiv: 2312.01728*, 2023.

[Qin and Wang, 2023] Rui Qin and Yong Wang. Imputegan: Generative adversarial network for multivariate time series imputation. *Entropy*, 25(1):137, 2023.

[Rajendran *et al.*, 2024] Goutham Rajendran, Simon Buchholz, Bryon Aragam, Bernhard Schölkopf, and Pradeep Ravikumar. Learning interpretable concepts: Unifying causal representation learning and foundation models. *arXiv preprint arXiv:2402.09236*, 2024.

[Rubin, 1976] Donald B Rubin. Inference and missing data. *Biometrika*, 63(3):581–592, 1976.

[Rubin, 1978] Donald B Rubin. Multiple imputations in sample surveys-a phenomenological bayesian approach to nonresponse. In *Proceedings of the survey research methods section of the American Statistical Association*, volume 1, pages 20–34. American Statistical Association Alexandria, VA, 1978.

[Schölkopf *et al.*, 2021] Bernhard Schölkopf, Francesco Locatello, Stefan Bauer, Nan Rosemary Ke, Nal Kalchbrenner, Anirudh Goyal, and Yoshua Bengio. Toward causal representation learning. *Proceedings of the IEEE*, 109(5):612–634, 2021.

[Simmons *et al.*, 2010] Deborah Simmons, Angela Hairrell, Meaghan Edmonds, Sharon Vaughn, Ross Larsen, Victor Willson, William Rupley, and Glenda Byrns. A comparison of multiple-strategy methods: Effects on fourth-grade students' general and content-specific reading comprehension and vocabulary development. *Journal of Research on Educational Effectiveness*, 3(2):121–156, 2010.

[Song *et al.*, 2024] Xiangchen Song, Weiran Yao, Yewen Fan, Xinshuai Dong, Guangyi Chen, Juan Carlos Niebles, Eric Xing, and Kun Zhang. Temporally disentangled representation learning under unknown nonstationarity. *Advances in Neural Information Processing Systems*, 36, 2024.

[Tang and Matteson, 2021] Binh Tang and David S Matteson. Probabilistic transformer for time series analysis. *Advances in Neural Information Processing Systems*, 34:23592–23608, 2021.

[Tashiro *et al.*, 2021] Yusuke Tashiro, Jiaming Song, Yang Song, and Stefano Ermon. Csci: Conditional score-based diffusion models for probabilistic time series imputation. *Advances in Neural Information Processing Systems*, 34:24804–24816, 2021.

[Van Buuren and Groothuis-Oudshoorn, 2011] Stef Van Buuren and Karin Groothuis-Oudshoorn. mice: Multivariate imputation by chained equations in r. *Journal of statistical software*, 45:1–67, 2011.

[Wendong *et al.*, 2024] Liang Wendong, Armin Kekić, Julius von Kügelgen, Simon Buchholz, Michel Besserve,

Luigi Gresele, and Bernhard Schölkopf. Causal component analysis. *Advances in Neural Information Processing Systems*, 36, 2024.

[Wu *et al.*, 2022] Haixu Wu, Tengge Hu, Yong Liu, Hang Zhou, Jianmin Wang, and Mingsheng Long. Timesnet: Temporal 2d-variation modeling for general time series analysis. *arXiv preprint arXiv:2210.02186*, 2022.

[Wu *et al.*, 2023] Haixu Wu, Hang Zhou, Mingsheng Long, and Jianmin Wang. Interpretable weather forecasting for worldwide stations with a unified deep model. *Nature Machine Intelligence*, 5(6):602–611, 2023.

[Xie *et al.*, 2023] Shaoan Xie, Lingjing Kong, Mingming Gong, and Kun Zhang. Multi-domain image generation and translation with identifiability guarantees. In *The Eleventh International Conference on Learning Representations*, 2023.

[Yan *et al.*, 2024] Hanqi Yan, Lingjing Kong, Lin Gui, Yuejie Chi, Eric Xing, Yulan He, and Kun Zhang. Counterfactual generation with identifiability guarantees. *Advances in Neural Information Processing Systems*, 36, 2024.

[Yao *et al.*, 2021] Weiran Yao, Yuewen Sun, Alex Ho, Changyin Sun, and Kun Zhang. Learning temporally causal latent processes from general temporal data. *arXiv preprint arXiv:2110.05428*, 2021.

[Yao *et al.*, 2022] Weiran Yao, Guangyi Chen, and Kun Zhang. Temporally disentangled representation learning. *Advances in Neural Information Processing Systems*, 35:26492–26503, 2022.

[Yao *et al.*, 2023] Dingling Yao, Danru Xu, Sébastien Lachapelle, Sara Magliacane, Perouz Taslakian, Georg Martius, Julius von Kügelgen, and Francesco Locatello. Multi-view causal representation learning with partial observability. *arXiv preprint arXiv:2311.04056*, 2023.

[Yoon *et al.*, 2018] Jinsung Yoon, William R Zame, and Mihuela van der Schaar. Estimating missing data in temporal data streams using multi-directional recurrent neural networks. *IEEE Transactions on Biomedical Engineering*, 66(5):1477–1490, 2018.

[Zhang and Chan, 2007] Kun Zhang and Laiwan Chan. Kernel-based nonlinear independent component analysis. In *International Conference on Independent Component Analysis and Signal Separation*, pages 301–308. Springer, 2007.

[Zhang *et al.*, 2021] Ying Zhang, Baohang Zhou, Xiangrui Cai, Wenyu Guo, Xiaoke Ding, and Xiaojie Yuan. Missing value imputation in multivariate time series with end-to-end generative adversarial networks. *Information Sciences*, 551:67–82, 2021.

[Zhang *et al.*, 2024] Kun Zhang, Shaoan Xie, Ignavier Ng, and Yujia Zheng. Causal representation learning from multiple distributions: A general setting. *arXiv preprint arXiv:2402.05052*, 2024.

[Zheng *et al.*, 2022] Yujia Zheng, Ignavier Ng, and Kun Zhang. On the identifiability of nonlinear ica: Sparsity and beyond. *Advances in neural information processing systems*, 35:16411–16422, 2022.

[Zhou *et al.*, 2021] Haoyi Zhou, Shanghang Zhang, Jieqi Peng, Shuai Zhang, Jianxin Li, Hui Xiong, and Wancai Zhang. Informer: Beyond efficient transformer for long sequence time-series forecasting. In *Proceedings of the AAAI conference on artificial intelligence*, volume 35, pages 11106–11115, 2021.

A Related Works

A.1 Time Series Imputation

In the field of statistics, Rubin’s seminal work in 1976 laid a critical foundation for traditional missing data processing by establishing a framework of procedures and conditions designed to mitigate the adverse effects of missing data [Rubin, 1976]. This theory underpins estimation methods such as Maximum Likelihood [Dempster *et al.*, 1977], introduced in 1977, and Multiple Imputation [Rubin, 1978], developed by Rubin in 1978. These methods ensure convergence to consistent estimates under the Missing at Random (MAR) assumption. However, most traditional approaches to handling missing data rely on the assumptions of Missing Completely at Random (MCAR) or MAR. For instance, [Gibb *et al.*, 2006] assumed data to be MCAR in their study. Similarly, [Simmons *et al.*, 2010] applied Multiple Imputation under the MAR assumption. [Grella *et al.*, 2008] employed the Maximum Observational Likelihood (IML) method to address missing data, which also relied on the MAR hypothesis. These traditional methods demonstrate robustness within their respective assumptions but may face limitations when the data deviates from these conditions, highlighting the need for more flexible approaches in modern data analysis.

Deep learning imputation methods have shown strong modelling capabilities for missing data imputation in recent years. The time series imputation method based on deep learning can be classified into several types: The RNN-based models use recurrent units to capture long-term temporal dependencies in time series [Che *et al.*, 2018; Yoon *et al.*, 2018]; the BRITS uses a bi-directional RNN, allowing the filled values to be updated efficiently during backpropagation [Cao *et al.*, 2018]; in terms of CNN-based models, this type of model most tends to discover periodicity in time series data using a 2D convolution kernel by transforming a 1D time series into a set of 2D tensors based on multiple cycles [Wu *et al.*, 2022]. Besides, some models select the GNN as the basement to learn the spatiotemporal representation of different channels in a multivariate time series through a message-passing graph neural network to reconstruct missing data. The model based on the self-attention mechanism [Cini *et al.*, 2021; Marisca *et al.*, 2022] not only captures the complex long-term dependencies well compared to the above models but also uses the global information to make reasonable inferences about the missing values and improves the accuracy of filling the missing values.

In addition, generative models are also standard for this task. The VAE-based generative model [Fortuin *et al.*, 2020; Mulyadi *et al.*, 2021; Kim *et al.*, 2023], which approximates the actual data distribution to reconstruct the missing values by maximizing the Evidence Lower Bound of the Marginal Likelihood (ELBO), while solving the problems of reliable confidence estimation and interpretability; on contrast, the GAN-based generative model [Luo *et al.*, 2018; Qin and Wang, 2023; Liu *et al.*, 2019; Miao *et al.*, 2021], which makes the generator able to simulate the actual data distribution to complete the data filling, by the adversarial training between the generator and the discriminator. Finally, the diffusion [Tashiro *et al.*, 2021; Alcaraz and Strothoff, 2022; Liu *et al.*, 2023a] based model. This model type captures complex data distributions by gradually adding and then inverting noise through a Markov chain of a series of diffusion steps to reconstruct missing values.

A.2 Identification

The independent component analysis (ICA) has been applied in various research to identify the causal representation [Rajendran *et al.*, 2024; Mansouri *et al.*, 2023; Wendong *et al.*, 2024], which aims to recover the latent variable with identification guarantees [Yao *et al.*, 2023; Schölkopf *et al.*, 2021; Liu *et al.*, 2023c; Gresle *et al.*, 2020]. Traditional methods often presuppose a linear interaction between latent and observed variables.[Comon, 1994; Hyvärinen, 2013; Lee and Lee, 1998; Zhang and Chan, 2007]. However, meeting the linear mixing process in real-world scenarios takes much work. Thus, different sorts of assumptions, such as sparse generation process and auxiliary variables, are adopted to facilitate identifiability in nonlinear ICA scenarios [Zheng *et al.*, 2022; Hyvärinen and Pajunen, 1999; Hyvärinen *et al.*, 2024; Khemakhem *et al.*, 2020b; Li *et al.*, 2023]. Expressly, identifiability is first confirmed by Aapo et al.’s research. In Ref. [Khemakhem *et al.*, 2020a; Hyvarinen and Morioka, 2016; Hyvarinen and Morioka, 2017; Hyvarinen *et al.*, 2019], they supposed that the exponential family consists of latent sources and introduced some variables like domain indexes, time indexes, and class labels as auxiliary variables. Besides, the research of Zhang et al. [Kong *et al.*, 2022; Xie *et al.*, 2023; Kong *et al.*, 2023; Yan *et al.*, 2024] shows that the component-wise identification for nonlinear ICA could be achieved without the exponential family assumption. Employ sparsity assumptions were applied in several types of research to achieve identifiability without any supervised signals [Zheng *et al.*, 2022; Hyvärinen and Pajunen, 1999; Hyvärinen *et al.*, 2024; Khemakhem *et al.*, 2020b; Li *et al.*, 2023]. For instance, [Lachapelle *et al.*, 2023; Lachapelle and Lacoste-Julien, 2022] propose to use mechanism sparsity regularization to identify causal latent variables. In Ref. [Zhang *et al.*, 2024] selected the sparse structures of latent variables. et al., aiming to achieve identifiability under distribution shift. In addition, to achieve identifiability of time series data, nonlinear ICA was also employed in Ref. [Hyvarinen and Morioka, 2016; Yan *et al.*, 2024; Huang *et al.*, 2023; Hälvä and Hyvarinen, 2020; Lippe *et al.*, 2022]. [Hyvarinen and Morioka, 2016] identify non-stationary time series data identifiability by premises and capitalize of variance changes across data segments based on independent sources. On the other hand, Permutation-based contrastive learning is employed to identify the latent variables in stationary time series data. Recently, some models applied independent noise and historical variability information, such as LEAP [Yao *et al.*, 2021] and TDRL [Yao *et al.*, 2022]. At the same time, [Song *et al.*, 2024] identified latent variables without the observed domain variables. In terms of the identifiability of modality, multimodal comparative learning was presented the identifiability by Imant et al. [Daunhawer *et al.*, 2023]. [Yao *et al.*, 2023] hypothesized that multi-perspective causal representations are recognizable in the case of par-

Dataset	Ratio	DMM-MAR		DMM-MNAR		TimeCIB		ImputeFormer		TimesNet		SAITS		GPVAE		CSDI		BRITS		SSGAN	
		MSE	MAE	MSE	MAE	MSE	MAE	MSE	MAE	MSE	MAE	MSE	MAE	MSE	MAE	MSE	MAE	MSE	MAE	MSE	MAE
ETTh1	0.2	0.121	0.225	0.138	0.248	0.208	0.339	0.262	0.244	0.158	0.255	0.164	0.274	0.160	0.285	0.520	0.367	0.117	0.250	0.149	0.281
	0.4	0.166	0.270	0.167	0.275	0.295	0.397	0.293	0.359	0.244	0.307	0.177	0.280	0.242	0.348	0.800	0.508	0.142	0.275	0.158	0.293
	0.6	0.197	0.297	0.210	0.313	0.389	0.444	0.304	0.374	0.346	0.365	0.214	0.305	0.344	0.412	0.855	0.550	0.249	0.353	0.219	0.338
ETTh2	0.2	0.105	0.220	0.135	0.252	0.266	0.226	0.199	0.313	0.124	0.230	0.164	0.288	0.357	0.438	0.530	0.415	0.248	0.373	0.185	0.329
	0.4	0.130	0.258	0.159	0.282	0.353	0.308	0.224	0.334	0.206	0.291	0.165	0.291	0.413	0.471	0.480	0.403	0.372	0.480	0.268	0.385
	0.6	0.186	0.301	0.307	0.381	0.443	0.353	0.221	0.339	0.269	0.331	0.391	0.412	0.512	0.528	0.770	0.522	0.367	0.464	0.527	0.571
ETTm1	0.2	0.040	0.130	0.042	0.137	0.092	0.217	0.092	0.207	0.092	0.190	0.050	0.145	0.078	0.197	0.044	0.136	0.041	0.136	0.046	0.147
	0.4	0.055	0.154	0.056	0.159	0.121	0.254	0.075	0.179	0.163	0.245	0.057	0.178	0.109	0.234	0.070	0.155	0.047	0.145	0.078	0.198
	0.6	0.059	0.159	0.067	0.160	0.167	0.307	0.109	0.213	0.263	0.310	0.064	0.165	0.155	0.283	0.120	0.177	0.063	0.170	0.078	0.194
ETTm2	0.2	0.030	0.108	0.076	0.176	0.188	0.249	0.078	0.195	0.059	0.159	0.064	0.165	0.200	0.338	0.042	0.126	0.105	0.230	0.100	0.221
	0.4	0.037	0.127	0.076	0.179	0.261	0.261	0.075	0.183	0.097	0.204	0.050	0.146	0.275	0.378	0.038	0.140	0.116	0.251	0.107	0.231
	0.6	0.047	0.145	0.105	0.212	0.350	0.348	0.095	0.218	0.148	0.246	0.079	0.202	0.395	0.463	0.073	0.168	0.183	0.316	0.172	0.298
Exchange	0.2	0.003	0.035	0.004	0.037	0.208	0.200	0.075	0.194	0.027	0.114	0.079	0.200	0.125	0.219	0.018	0.087	0.508	0.608	0.361	0.523
	0.4	0.007	0.051	0.080	0.218	0.216	0.297	0.078	0.198	0.034	0.130	0.126	0.269	0.419	0.362	0.063	0.144	0.633	0.680	0.399	0.525
	0.6	0.006	0.052	0.014	0.076	0.295	0.432	0.087	0.211	0.039	0.143	0.146	0.297	0.508	0.401	0.055	0.150	0.783	0.750	0.576	0.658
Weather	0.2	0.036	0.062	0.039	0.064	0.046	0.108	0.065	0.121	0.041	0.091	0.041	0.076	0.048	0.099	0.061	0.065	0.035	0.077	0.040	0.072
	0.4	0.037	0.067	0.040	0.076	0.052	0.119	0.058	0.115	0.051	0.111	0.046	0.087	0.056	0.113	0.064	0.069	0.037	0.080	0.041	0.082
	0.6	0.043	0.073	0.046	0.085	0.066	0.138	0.063	0.121	0.066	0.131	0.056	0.101	0.069	0.132	0.070	0.075	0.046	0.097	0.053	0.099

Table 4: Experiment results in supervised scenarios for various datasets with different missing ratios under Missing At Random (MAR) conditions.

tial observations. In this article, based on multi-modality time series data, the fairness of multi-modality data and variability historical information was leveraged to prove the identifiability.

B Data Preprocessing

B.1 Simulation Experiment

Simulation Data Generation Process. As for the temporally latent processes, we use MLPs with the activation function of LeakyReLU to model the time-delayed of temporally latent variables. For all datasets, we set sequence length as 5 and transition lag as 1. That is:

$$z_{t,i} = (\text{LeakyReLU}(W_{i,:} \cdot \mathbf{z}_{t-1}, 0.2) + V_{<i,i} \cdot \mathbf{z}_{t,<i}) \cdot \epsilon_{t,i} + \epsilon_{t,i},$$

where $W_{i,:}$ is the i -th row of W and $V_{<i,i}$ is the first $i-1$ columns in the i -th row of V . Moreover, each independent noise $\epsilon_{t,i}$ is sampled from the distribution of normal distribution. We further let the data generation process from latent variables to observed variables be MLPs with the LeakyReLU units.

We provide a synthetic dataset A, with 3 latent variables. For dataset A, we have $W_A = [[1, 1, 0], [0, 1, 0], [0, 0, 1]]$. When it comes to V , we have and only have $V_{i-1,i} = 1 \ \forall i > 0$ for dataset A. The total size of the dataset is 100,000, with 1,024 samples designated as the validation set. The remaining samples are the training set.

Evaluation Metrics. To evaluate the identifiability performance of our method under instantaneous dependencies, we employ the Mean Correlation Coefficient (MCC) between the ground-truth \mathbf{z}_t and the estimated $\hat{\mathbf{z}}_t$. A higher MCC denotes a better identification performance the model can achieve. In addition, we also draw the estimated latent causal process to validate our method. Since the estimated transition function will be a transformation of the ground truth, we do not compare their exact values, but only the activated entries.

Experiment Results. We have provided the MCC results for missing cause variable **c** in Table 12. Additionally, we performed a comprehensive sensitivity analysis of the loss function coefficients to facilitate a systematic comparison between temporal latent variables and missing causes, in Table 14.

B.2 Real-world Experiments

Dataset. To evaluate the performance of the proposed method, we consider the following datasets: 1) **ETT** [Zhou *et al.*, 2021] is an electricity transformer temperature dataset collected from two separated counties in China, including four different datasets {ETTh1, ETTh2, ETTm1, ETTm2}; 2) **Exchange** [Lai *et al.*, 2018] is the daily exchange rate dataset from of eight foreign countries including Australia, British, Canada, Switzerland, China, Japan, New Zealand, and Singapore ranging from 1990 to 2016; 3) **Weather**⁴ is recorded at the Weather Station at the Max Planck Institute for Biogeochemistry in Jena, Germany. 4) **MIMIC-III**⁵ [Johnson *et al.*, 2016] is a published dataset with de-identified health-related data associated with more than forty thousand patients who stayed in critical care units of the Beth Israel Deaconess Medical Center between 2001 and 2012. For each dataset, we generate mask matrices to simulate missing values based on the missing mechanisms of MAR and MNAR. Meanwhile, we use three different mask ratios, such as 0.2, 0.4, and 0.6. In addition, we use both supervised learning and unsupervised learning methods for training. Supervised learning provides missing data during the model training phase to calculate the loss and optimize the model, while unsupervised learning does not provide missing data. However, in order to improve the filling performance of the model, the observed data is partially masked during unsupervised learning and provided during model training to calculate the loss.

⁴<https://www.bgc-jena.mpg.de/wetter/>

⁵<https://mimic.mit.edu/docs/gettingstarted/>

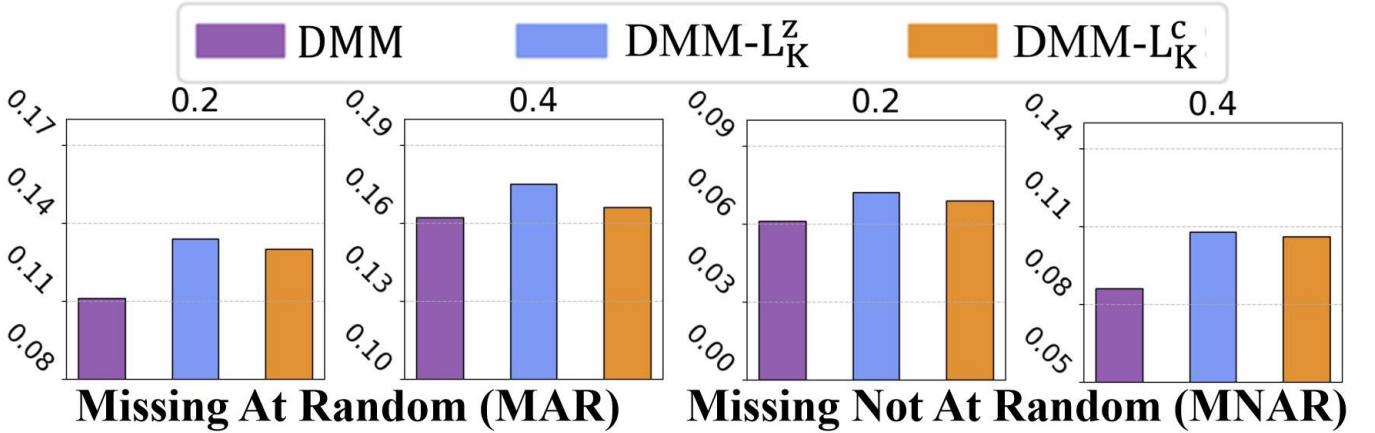


Figure 3: Ablation study on the ETTh1 datasets.

Data Preprocessing. To facilitate the training of the dataset, we introduce a mask matrix R , to denote the missing positions in the time series data. Consequently, the representation of the time series data, as defined by R , is as follows:

$$X = R * X^o + (1 - R) * X^m \quad (23)$$

Depending on the two distinct data missing mechanisms, we can generate various mask matrices R .

Generation of mask matrix R under MAR. Randomly select a certain proportion of data from the complete data X as the estimated observable data \hat{X}^o , and the remaining data is the estimated missing data \hat{X}^m . At this time, the estimated mask matrix is denoted as \hat{R} . After passing \hat{X}^o through an MLP, a mask matrix \hat{R}^o is generated. Since the missing data depends on the complete variables rather than the missing data itself, the positions where \hat{R} and \hat{R}^o are both non-zero can be considered as missing data that does not depend on themselves. The mask matrix can be generated as follows:

$$R = 1 - (1 - \hat{R}) \odot (1 - \hat{R}^o) \quad (24)$$

Generation of mask matrix R under MNAR. Missing Not At Random refers to situations other than Missing Completely At Random and Missing At Random. Specifically, data loss is necessarily related to missing variables and may also be related to complete data. According to the causal diagram, we know that the missing cause at the current moment is caused by the temporal data of the previous moments. Therefore, we input the data of the previous moments into an MLP to construct the mask matrix R_t for this moment, that is, $R_t = m(X_{t-1})$. The MLP is not randomly initialized but manually verified. We use the MLP to estimate missingness probabilities for the rest and generate the mask by ranking these values to match the desired missing rate. We repeat the process if the mask doesn't meet the criteria.

Experiment Results. For each experimental configuration, we conducted three independent trials with varying random seeds and reported the mean and standard deviation of the results. The results of our supervised learning experiments are tabulated in Table 4 and Table 5. We reported the standard deviation of all experiments in Table 8, Table 9, Table 10 and Table 11. In some real-world scenarios, missingness may depend on future information. While our original assumption focused on past dependencies, we have added a new experiment on the Exchange dataset under an MNAR setting where the mask depends on past, present, and future data (see Table 13). Furthermore, we provide experimental results obtained from the MIMIC-III medical dataset, which are illustrated in Table 15.

Mixed Missing Mechanisms. We added experiments under mixed missingness settings with different MCAR:MAR:MNAR ratios (Table 16). Our model performs well across settings, though performance slightly drops when MCAR dominates due to its randomness.

B.3 Ablation Study

We constructed two different model variants for both MAR and MNAR scenarios: a) $DMM-L_K^z$: We eliminate the latent state prior along with the associated Kullback-Leibler (KL) divergence term from the model. b) $DMM-L_K^c$: We eliminate the missing cause prior and its associated Kullback-Leibler (KL) divergence term from our model. Experiment results on the ETTh1 dataset are shown in Figure 3. Our experiments revealed that the elimination of either the latent state prior or the missing cause prior led to a decline in model performance. This underscores the importance of these priors in the imputation process, suggesting that they are capable of encapsulating temporal information.

B.4 Model Efficiency

We evaluate the performance of our model and the baseline model on the ETTh2 dataset from three aspects: imputation performance, training speed, and memory footprint, as shown in Figure 6. Compared with other models for time-series imputation, we can find that the proposed DMM has the best model performance and relatively good model efficiency.

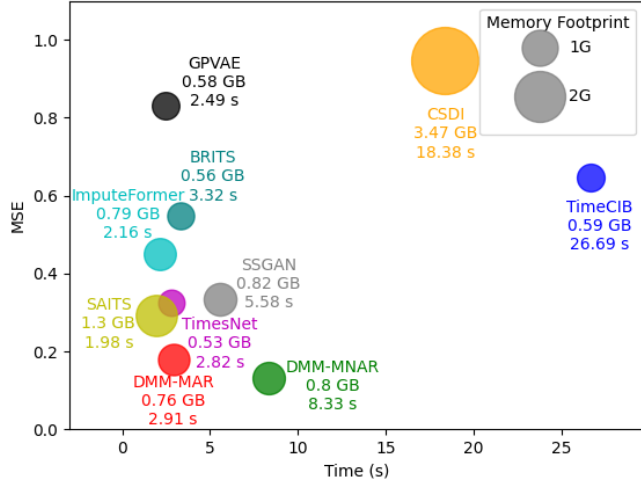


Figure 4: Computational efficiency of ETTh2 dataset with a missing rate of 0.6 under unsupervised conditions in MNAR

C Proof

Theorem 1. (Identification of Latent States and Missing Causes under MAR.) Suppose that the observed data from missing time series data is generated following the data generation process, and we make the following assumptions:

- A1 (Smooth, Positive and Conditional independent Density:) [Yao et al., 2022; Yao et al., 2021] The probability density function of latent variables is smooth and positive, i.e., $p(\mathbf{z}_t|\mathbf{z}_{t-1}) > 0$, $p(\mathbf{c}_t|\mathbf{x}_t^o) > 0$. Conditioned on \mathbf{z}_{t-1} each $z_{t,i}$ is independent of any other $z_{t,j}$ for $i, j \in 1, \dots, n, i \neq j$, i.e., $\log p(\mathbf{z}_t|\mathbf{z}_{t-1}) = \sum_{k=1}^n \log p(z_{t,k}|\mathbf{z}_{t-1})$. Conditioned on \mathbf{x}^o each $c_{t,i}$ is independent of any other $c_{t,j}$ for $i, j \in 1, \dots, n, i \neq j$, i.e., $\log p(\mathbf{c}_t|\mathbf{x}_t^o) = \sum_{k=1}^n \log p(c_{t,k}|\mathbf{x}_t^o)$.

- A2 (Linear Independent of MAR:) [Yao et al., 2022] For any \mathbf{z}_t , there exist $2n + 1$ values of $z_{t-1,l}$, $l = 1, \dots, n$, such that these $2n$ vectors $\mathbf{v}_{t,k,l}^A - \mathbf{v}_{t,k,n}^A$ are linearly independent, where $\mathbf{v}_{t,k,l}^A$ is defined as follows:

$$\mathbf{v}_{t,k,l}^A = \left(\frac{\partial^2 \log p(z_{t,k}|\mathbf{z}_{t-1})}{\partial z_{t,k} \partial z_{t-1,1}}, \dots, \frac{\partial^2 \log p(z_{t,k}|\mathbf{z}_{t-1})}{\partial z_{t,k} \partial z_{t-1,n}}, \frac{\partial^3 \log p(z_{t,k}|\mathbf{z}_{t-1})}{\partial^2 z_{t,k} \partial z_{t-1,1}}, \dots, \frac{\partial^3 \log p(z_{t,k}|\mathbf{z}_{t-1})}{\partial^2 z_{t,k} \partial z_{t-1,n}} \right)^T$$

Similarly, for each value of \mathbf{c}_t , there exist $2n + 1$ values of \mathbf{x}_t^o , i.e., $\mathbf{x}_{t,j}^o$ with $j = 0, 2, \dots, 2n$, such that these $2n$ vectors $\mathbf{w}^A(\mathbf{c}_t, \mathbf{x}_{t,j}^o) - \mathbf{w}^A(\mathbf{c}_t, \mathbf{x}_{t,0}^o)$ are linearly independent, where the vector $\mathbf{w}^A(\mathbf{c}_t, \mathbf{x}_{t,j}^o)$ is defined as follows:

$$\mathbf{w}^A(\mathbf{c}_t, \mathbf{x}_{t,j}^o) = \left(\frac{\partial^2 \log p(c_{t,k}|\mathbf{x}_t^o)}{\partial^2 c_{t,k}}, \dots, \frac{\partial^2 \log p(c_{t,k}|\mathbf{x}_t^o)}{\partial^2 c_{t,k}}, \frac{\partial \log p(c_{t,k}|\mathbf{x}_t^o)}{\partial c_{t,k}}, \dots, \frac{\partial \log p(c_{t,k}|\mathbf{x}_t^o)}{\partial c_{t,k}} \right)^T$$

Then, by learning the data generation process, \mathbf{z}_t and \mathbf{c}_t are component-wise identifiable.

Proof. We start from the matched marginal distribution to develop the relation between \mathbf{z}_t and $\hat{\mathbf{z}}_t$ as follows:

$$p(\hat{\mathbf{x}}_t) = p(\mathbf{x}_t) \iff p(\hat{g}(\hat{\mathbf{z}}_t)) = p(g(\mathbf{z}_t)) \iff p(g^{-1} \circ \hat{g}(\hat{\mathbf{z}}_t)) = p(\mathbf{z}_t) |\mathbf{J}_{g^{-1}}^A| \iff p(h(\hat{\mathbf{z}}_t)) = p(\mathbf{z}_t),$$

where $\hat{g}^{-1} : \mathcal{X} \rightarrow \mathcal{Z}$ denotes the estimated invertible generation function, and $h := g^{-1} \circ \hat{g}$ is the transformation between the true latent variables and the estimated one. $|\mathbf{J}_{g^{-1}}^A|$ denotes the absolute value of Jacobian matrix determinant of g^{-1} . Note that as both \hat{g}^{-1} and g are invertible, $|\mathbf{J}_{g^{-1}}^A| \neq 0$ and h is invertible.

The Jacobian matrix of the mapping from $(\mathbf{x}_{t-1}, \hat{\mathbf{z}}_t)$ to $(\mathbf{x}_{t-1}, \mathbf{z}_t)$ is

$$\begin{bmatrix} \mathbf{I} & \mathbf{0} \\ * & \mathbf{J}_h^A \end{bmatrix},$$

where $*$ denotes a matrix, and the determinant of this Jacobian matrix is $|\mathbf{J}_h^A|$. Since \mathbf{x}_{t-1} do not contain any information of $\hat{\mathbf{z}}_t$, the right-top element is $\mathbf{0}$. Therefore $p(\hat{\mathbf{z}}_t, \mathbf{x}_{t-1}) = p(\mathbf{z}_t, \mathbf{x}_{t-1}) \cdot |\mathbf{J}_h^A|$. Dividing both sides of this equation by $p(\mathbf{x}_{t-1})$ gives

$$p(\hat{\mathbf{z}}_t|\mathbf{x}_{t-1}) = p(\mathbf{z}_t|\mathbf{x}_{t-1}) \cdot |\mathbf{J}_h^A| \quad (25)$$

Since $p(\mathbf{z}_t|\mathbf{z}_{t-1}) = p(\mathbf{z}_t|g(\mathbf{z}_{t-1})) = p(\mathbf{z}_t|\mathbf{x}_{t-1})$ and similarly $p(\hat{\mathbf{z}}_t|\hat{\mathbf{z}}_{t-1}) = p(\hat{\mathbf{z}}_t|\mathbf{x}_{t-1})$, we have

$$\log p(\hat{\mathbf{z}}_t|\hat{\mathbf{z}}_{t-1}) = \log p(\mathbf{z}_t|\mathbf{z}_{t-1}) + \log |\mathbf{J}_h^A| = \sum_{k=1}^n \log p(z_{t,k}|\mathbf{z}_{t-1}) + \log |\mathbf{J}_h^A| \quad (26)$$

Dataset	Ratio	DMM-MAR		DMM-MNAR		TimeCIB		ImputeFormer		TimesNet		SAITS		GPVAE		CSDI		BRITS		SSGAN	
		MSE	MAE	MSE	MAE	MSE	MAE	MSE	MAE	MSE	MAE	MSE	MAE	MSE	MAE	MSE	MAE	MSE	MAE	MSE	MAE
ETTh1	0.2	0.090	0.190	0.061	0.164	0.165	0.306	0.282	0.346	0.089	0.199	0.075	0.173	0.142	0.282	0.221	0.249	0.121	0.250	0.144	0.276
	0.4	0.106	0.209	0.086	0.195	0.216	0.349	0.377	0.398	0.144	0.249	0.096	0.207	0.186	0.319	0.415	0.340	0.148	0.275	0.168	0.294
	0.6	0.156	0.259	0.144	0.252	0.284	0.394	0.502	0.456	0.223	0.305	0.150	0.258	0.276	0.385	0.613	0.439	0.247	0.365	0.241	0.355
ETTh2	0.2	0.083	0.189	0.081	0.185	0.192	0.217	0.183	0.309	0.096	0.218	0.100	0.224	0.361	0.458	0.241	0.277	0.187	0.332	0.203	0.346
	0.4	0.096	0.207	0.091	0.203	0.213	0.329	0.207	0.328	0.146	0.252	0.150	0.270	0.370	0.451	0.226	0.289	0.235	0.361	0.285	0.382
	0.6	0.116	0.228	0.112	0.226	0.247	0.302	0.220	0.336	0.205	0.296	0.200	0.328	0.474	0.508	0.388	0.373	0.459	0.318	0.424	
ETTm1	0.2	0.031	0.120	0.026	0.101	0.079	0.206	0.076	0.189	0.060	0.158	0.039	0.136	0.063	0.180	0.028	0.105	0.040	0.133	0.061	0.168
	0.4	0.032	0.117	0.029	0.111	0.104	0.242	0.135	0.252	0.101	0.203	0.056	0.165	0.085	0.211	0.038	0.116	0.047	0.146	0.075	0.191
	0.6	0.045	0.141	0.042	0.132	0.146	0.289	0.095	0.207	0.167	0.255	0.088	0.209	0.123	0.256	0.065	0.143	0.063	0.172	0.074	0.191
ETTm2	0.2	0.039	0.124	0.037	0.123	0.154	0.178	0.109	0.244	0.047	0.140	0.095	0.217	0.109	0.245	0.034	0.148	0.103	0.235	0.108	0.243
	0.4	0.048	0.144	0.048	0.143	0.186	0.193	0.133	0.268	0.075	0.179	0.179	0.291	0.115	0.247	0.052	0.152	0.118	0.251	0.107	0.241
	0.6	0.061	0.161	0.054	0.151	0.237	0.202	0.137	0.270	0.110	0.221	0.224	0.326	0.260	0.347	0.076	0.166	0.209	0.329	0.189	0.325
Exchange	0.2	0.004	0.036	0.002	0.034	0.207	0.291	0.110	0.249	0.025	0.112	0.138	0.283	0.159	0.157	0.016	0.086	0.465	0.577	0.338	0.504
	0.4	0.009	0.053	0.007	0.052	0.260	0.320	0.105	0.252	0.032	0.128	0.140	0.304	0.189	0.173	0.024	0.104	0.645	0.673	0.405	0.552
	0.6	0.006	0.059	0.006	0.054	0.376	0.416	0.104	0.247	0.039	0.141	0.224	0.378	0.214	0.226	0.029	0.117	0.829	0.786	0.684	0.724
Weather	0.2	0.046	0.078	0.030	0.048	0.045	0.103	0.072	0.131	0.037	0.080	0.035	0.065	0.051	0.099	0.059	0.069	0.036	0.077	0.039	0.069
	0.4	0.038	0.063	0.036	0.059	0.050	0.113	0.068	0.130	0.043	0.093	0.039	0.074	0.054	0.113	0.062	0.067	0.039	0.081	0.042	0.082
	0.6	0.052	0.092	0.042	0.071	0.061	0.131	0.072	0.138	0.054	0.111	0.045	0.089	0.065	0.128	0.071	0.081	0.047	0.093	0.049	0.097

Table 5: Experiment results in supervised scenarios for various datasets with different missing ratios under Missing Not At Random (MNAR) conditions.

For $i, j \in \{1, \dots, n\}$, $i \neq j$, conditioned on \mathbf{z}_{t-1} each $z_{t,i}$ is independent of any other $z_{t,j}$, we have:

$$\frac{\partial^2 \log p(\hat{\mathbf{z}}_t | \hat{\mathbf{z}}_{t-1})}{\partial \hat{z}_{t,i} \partial \hat{z}_{t,j}} = 0 \quad (27)$$

Sequentially, the first-order derivative w.r.t. $\hat{z}_{t,i}$ is

$$\frac{\partial \log p(\hat{\mathbf{z}}_t | \hat{\mathbf{z}}_{t-1})}{\partial \hat{z}_{t,i}} = \sum_{k=1}^n \frac{\partial \log p(z_{t,k} | \mathbf{z}_{t-1})}{\partial z_{t,k}} \cdot \frac{\partial z_{t,k}}{\partial \hat{z}_{t,i}} + \frac{\partial \log |\mathbf{J}_h^A|}{\partial \hat{z}_{t,i}} \quad (28)$$

Sequentially, we conduct the second-order derivative w.r.t. $\hat{z}_{t,j}, \hat{z}_{t,j}$ and have

$$\frac{\partial^2 \log p(\hat{\mathbf{z}}_t | \hat{\mathbf{z}}_{t-1})}{\partial \hat{z}_{t,i} \partial \hat{z}_{t,j}} = \sum_{k=1}^n \left(\frac{\partial^2 \log p(z_{t,k} | \mathbf{z}_{t-1})}{\partial^2 z_{t,k}} \cdot \frac{\partial z_{t,k}}{\partial \hat{z}_{t,i}} \cdot \frac{\partial z_{t,k}}{\partial \hat{z}_{t,j}} + \frac{\partial \log p(z_{t,k} | \mathbf{z}_{t-1})}{\partial z_{t,k}} \cdot \frac{\partial^2 z_{t,k}}{\partial \hat{z}_{t,i} \partial \hat{z}_{t,j}} \right) + \frac{\partial^2 \log |\mathbf{J}_h^A|}{\partial \hat{z}_{t,i} \partial \hat{z}_{t,j}} \quad (29)$$

According to Equation 27 and the fact that \mathbf{h}_t does not depend on $z_{t-1,l}$ for each $l = 1, \dots, n$, that is

$$\sum_{k=1}^n \left(\frac{\partial^3 \log p(z_{t,k} | \mathbf{z}_{t-1})}{\partial^2 z_{t,k} \partial z_{t-1,l}} \cdot \frac{\partial z_{t,k}}{\partial \hat{z}_{t,i}} \cdot \frac{\partial z_{t,k}}{\partial \hat{z}_{t,j}} + \frac{\partial^2 \log p(z_{t,k} | \mathbf{z}_{t-1})}{\partial z_{t,k} \partial z_{t-1,l}} \cdot \frac{\partial^2 z_{t,k}}{\partial \hat{z}_{t,i} \partial \hat{z}_{t,j}} \right) = 0 \quad (30)$$

For each value of \mathbf{z}_t , $\mathbf{v}_{t,k,l}^A - \mathbf{v}_{t,k,n}^A$ are linearly independents, so $\frac{\partial z_{t,k}}{\partial \hat{z}_{t,i}} \cdot \frac{\partial z_{t,k}}{\partial \hat{z}_{t,j}} = 0$. That is, in each row of \mathbf{J}_h^A there is only one non-zero entry. Since \mathbf{h} is invertible, then \mathbf{z}_t is component-wise identifiable.

Similarly, we have $p(h_c(\hat{\mathbf{c}}_t)) = p(\mathbf{c}_t)$, then

$$\log p(\hat{\mathbf{c}}_t | \mathbf{x}_t^o) = \log p(\mathbf{c}_t | \mathbf{x}_t^o) + \log |\mathbf{J}_{h_c}^A| = \sum_{k=1}^n \log p(c_{t,k} | \mathbf{x}_t^o) + \log |\mathbf{J}_{h_c}^A| \quad (31)$$

For $i, j \in \{1, \dots, n\}$, $i \neq j$, conditioned on \mathbf{x}_t^o each $c_{t,i}$ is independent of any other $c_{t,j}$, we have:

$$\frac{\partial^2 \log p(\hat{\mathbf{c}}_t | \mathbf{x}_t^o)}{\partial \hat{c}_{t,i} \partial \hat{c}_{t,j}} = 0 \quad (32)$$

Sequentially, the first-order derivative w.r.t. $\hat{c}_{t,i}$ is

$$\frac{\partial \log p(\hat{\mathbf{c}}_t | \mathbf{x}_t^o)}{\partial \hat{c}_{t,i}} = \sum_{k=1}^n \frac{\partial \log p(c_{t,k} | \mathbf{x}_t^o)}{\partial c_{t,k}} \cdot \frac{\partial c_{t,k}}{\partial \hat{c}_{t,i}} + \frac{\partial \log |\mathbf{J}_{h_c}^A|}{\partial \hat{c}_{t,i}} \quad (33)$$

Sequentially, we conduct the second-order derivative w.r.t. $\hat{c}_{t,j}, \hat{c}_{t,j}$ and have

$$\frac{\partial^2 \log p(\hat{\mathbf{c}}_t | \mathbf{x}_t^o)}{\partial \hat{c}_{t,i} \partial \hat{c}_{t,j}} = \sum_{k=1}^n \left(\frac{\partial^2 \log p(c_{t,k} | \mathbf{x}_t^o)}{\partial^2 c_{t,k}} \cdot \frac{\partial c_{t,k}}{\partial \hat{c}_{t,i}} \cdot \frac{\partial c_{t,k}}{\partial \hat{c}_{t,j}} + \frac{\partial \log p(c_{t,k} | \mathbf{x}_t^o)}{\partial c_{t,k}} \cdot \frac{\partial^2 c_{t,k}}{\partial \hat{c}_{t,i} \partial \hat{c}_{t,j}} \right) + \frac{\partial^2 \log |\mathbf{J}_{h_c}^A|}{\partial \hat{c}_{t,i} \partial \hat{c}_{t,j}} \quad (34)$$

Therefore, there exist $2n + 1$ values of \mathbf{x}_t^o , i.e., $\mathbf{x}_{t,l}^o$ with $l = 0, 2, \dots, 2n$, we have $2n + 1$ such equations. Subtracting each equation corresponding to $\mathbf{x}_{t,1}^o \dots \mathbf{x}_{t,2n}^o$ with the equation corresponding to $\mathbf{x}_{t,0}^o$ results in $2n$ equations:

$$\sum_{k=1}^n \left(\left(\frac{\partial^2 \log p(c_{t,k} | \mathbf{x}_{t,l}^o)}{\partial^2 c_{t,k}} - \frac{\partial^2 \log p(c_{t,k} | \mathbf{x}_{t,0}^o)}{\partial^2 c_{t,k}} \right) \cdot \frac{\partial c_{t,k}}{\partial \hat{c}_{t,i}} \cdot \frac{\partial c_{t,k}}{\partial \hat{c}_{t,j}} + \left(\frac{\partial \log p(c_{t,k} | \mathbf{x}_{t,l}^o)}{\partial c_{t,k}} - \frac{\partial \log p(c_{t,k} | \mathbf{x}_{t,0}^o)}{\partial c_{t,k}} \right) \cdot \frac{\partial^2 c_{t,k}}{\partial \hat{c}_{t,i} \partial \hat{c}_{t,j}} \right) = 0 \quad (35)$$

under the linear independence condition in Assumption A2, we have $\frac{\partial c_{t,k}}{\partial c_{t,i}} \cdot \frac{\partial c_{t,k}}{\partial c_{t,j}} = 0$. That is, in each row of $\mathbf{J}_{h_c}^A$ there is only one non-zero entry. Since h_c is invertible, then \mathbf{c}_t is component-wise identifiable. \square

Theorem 2. (Identification of Latent States and Missing Causes under MNAR.) We follow the A1 in Theorem 1 and suppose that the observed data from missing time series data is generated following the data generation process, and we further make the following assumptions:

- A3 (**Linear Independence of MNAR:**) [Yao et al., 2022] For any \mathbf{z}_t , there exist $2n + 1$ values of $z_{t-1,l}, l = 1, \dots, n$, such that these $2n$ vectors $\mathbf{v}_{t,k,l}^B - \mathbf{v}_{t,k,n}^B$ are linearly independent, where $\mathbf{v}_{t,k,l}^B$ is defined as follows:

$$\mathbf{v}_{t,k,l}^B = \left(\frac{\partial^2 \log p(z_{t,k} | \mathbf{z}_{t-1})}{\partial z_{t,k} \partial z_{t-1,1}}, \dots, \frac{\partial^2 \log p(z_{t,k} | \mathbf{z}_{t-1})}{\partial z_{t,k} \partial z_{t-1,n}}, \frac{\partial^3 \log p(z_{t,k} | \mathbf{z}_{t-1})}{\partial^2 z_{t,k} \partial z_{t-1,1}}, \dots, \frac{\partial^3 \log p(z_{t,k} | \mathbf{z}_{t-1})}{\partial^2 z_{t,k} \partial z_{t-1,n}} \right)^T$$

Similarly, for each value of \mathbf{c}_t , there exist $2n + 1$ values of \mathbf{x}_{t-1} , i.e., $\mathbf{x}_{t-1,j}$ with $j = 0, 2, \dots, 2n$, such that these $2n$ vectors $\mathbf{w}^B(\mathbf{c}_t, \mathbf{x}_{t-1,j}) - \mathbf{w}^B(\mathbf{c}_t, \mathbf{x}_{t-1,0})$ are linearly independent, where the vector $\mathbf{w}^B(\mathbf{c}_t, \mathbf{x}_{t-1,j})$ is defined as follows:

$$\mathbf{w}^B(\mathbf{c}_t, \mathbf{x}_{t-1,j}) = \left(\frac{\partial^2 \log p(c_{t,k} | \mathbf{x}_{t-1})}{\partial^2 c_{t,k}}, \dots, \frac{\partial^2 \log p(c_{t,k} | \mathbf{x}_{t-1})}{\partial^2 c_{t,k}}, \frac{\partial \log p(c_{t,k} | \mathbf{x}_{t-1})}{\partial c_{t,k}}, \dots, \frac{\partial \log p(c_{t,k} | \mathbf{x}_{t-1})}{\partial c_{t,k}} \right)^T$$

Then, by learning the data generation process, \mathbf{z}_t and \mathbf{c}_t are component-wise identifiable.

Proof. We start from the matched marginal distribution to develop the relation between \mathbf{z}_t and $\hat{\mathbf{z}}_t$ as follows:

$$p(\hat{\mathbf{x}}_t) = p(\mathbf{x}_t) \iff p(\hat{g}(\hat{\mathbf{z}}_t)) = p(g(\mathbf{z}_t)) \iff p(g^{-1} \circ \hat{g}(\hat{\mathbf{z}}_t)) = p(\mathbf{z}_t) | \mathbf{J}_{g^{-1}}^B | \iff p(h(\hat{\mathbf{z}}_t)) = p(\mathbf{z}_t),$$

where $\hat{g}^{-1} : \mathcal{X} \rightarrow \mathcal{Z}$ denotes the estimated invertible generation function, and $h := g^{-1} \circ \hat{g}$ is the transformation between the true latent variables and the estimated one. $|\mathbf{J}_{g^{-1}}^B|$ denotes the absolute value of Jacobian matrix determinant of g^{-1} . Note that as both \hat{g}^{-1} and g are invertible, $|\mathbf{J}_{g^{-1}}^B| \neq 0$ and h is invertible.

The Jacobian matrix of the mapping from $(\mathbf{x}_{t-1}, \hat{\mathbf{z}}_t)$ to $(\mathbf{x}_{t-1}, \mathbf{z}_t)$ is

$$\begin{bmatrix} \mathbf{I} & \mathbf{0} \\ * & \mathbf{J}_h^B \end{bmatrix},$$

where $*$ denotes a matrix, and the determinant of this Jacobian matrix is $|\mathbf{J}_h^B|$. Since \mathbf{x}_{t-1} do not contain any information of $\hat{\mathbf{z}}_t$, the right-top element is $\mathbf{0}$. Therefore $p(\hat{\mathbf{z}}_t, \mathbf{x}_{t-1}) = p(\mathbf{z}_t, \mathbf{x}_{t-1}) \cdot |\mathbf{J}_h^B|$. Dividing both sides of this equation by $p(\mathbf{x}_{t-1})$ gives

$$p(\hat{\mathbf{z}}_t | \mathbf{x}_{t-1}) = p(\mathbf{z}_t | \mathbf{x}_{t-1}) \cdot |\mathbf{J}_h^B| \quad (36)$$

Since $p(\mathbf{z}_t | \mathbf{z}_{t-1}) = p(\mathbf{z}_t | g(\mathbf{z}_{t-1})) = p(\mathbf{z}_t | \mathbf{x}_{t-1})$ and similarly $p(\hat{\mathbf{z}}_t | \hat{\mathbf{z}}_{t-1}) = p(\hat{\mathbf{z}}_t | \mathbf{x}_{t-1})$, we have

$$\log p(\hat{\mathbf{z}}_t | \hat{\mathbf{z}}_{t-1}) = \log p(\mathbf{z}_t | \mathbf{z}_{t-1}) + \log |\mathbf{J}_h^B| = \sum_{k=1}^n \log p(z_{t,k} | \mathbf{z}_{t-1}) + \log |\mathbf{J}_h^B| \quad (37)$$

For $i, j \in \{1, \dots, n\}$, $i \neq j$, conditioned on \mathbf{z}_{t-1} each $z_{t,i}$ is independent of any other $z_{t,j}$, we have:

$$\frac{\partial^2 \log p(\hat{\mathbf{z}}_t | \hat{\mathbf{z}}_{t-1})}{\partial \hat{z}_{t,i} \partial \hat{z}_{t,j}} = 0 \quad (38)$$

Sequentially, the first-order derivative w.r.t. $\hat{z}_{t,i}$ is

$$\frac{\partial \log p(\hat{\mathbf{z}}_t | \hat{\mathbf{z}}_{t-1})}{\partial \hat{z}_{t,i}} = \sum_{k=1}^n \frac{\partial \log p(z_{t,k} | \mathbf{z}_{t-1})}{\partial z_{t,k}} \cdot \frac{\partial z_{t,k}}{\partial \hat{z}_{t,i}} + \frac{\partial \log |\mathbf{J}_h^B|}{\partial \hat{z}_{t,i}} \quad (39)$$

Sequentially, we conduct the second-order derivative w.r.t $\hat{z}_{t,j}, \hat{z}_{t,j}$ and have

$$\frac{\partial^2 \log p(\hat{\mathbf{z}}_t | \hat{\mathbf{z}}_{t-1})}{\partial \hat{z}_{t,i} \partial \hat{z}_{t,j}} = \sum_{k=1}^n \left(\frac{\partial^2 \log p(z_{t,k} | \mathbf{z}_{t-1})}{\partial^2 z_{t,k}} \cdot \frac{\partial z_{t,k}}{\partial \hat{z}_{t,i}} \cdot \frac{\partial z_{t,k}}{\partial \hat{z}_{t,j}} + \frac{\partial \log p(z_{t,k} | \mathbf{z}_{t-1})}{\partial z_{t,k}} \cdot \frac{\partial^2 z_{t,k}}{\partial \hat{z}_{t,i} \partial \hat{z}_{t,j}} \right) + \frac{\partial^2 \log |\mathbf{J}_h^B|}{\partial \hat{z}_{t,i} \partial \hat{z}_{t,j}} \quad (40)$$

According to Equation 38 and the fact that h does not depend on $z_{t-1,l}$ for each $l = 1, \dots, n$, that is

$$\sum_{k=1}^n \left(\frac{\partial^2 \log p(z_{t,k} | \mathbf{z}_{t-1})}{\partial^2 z_{t,k}} \cdot \frac{\partial z_{t,k}}{\partial \hat{z}_{t,i}} \cdot \frac{\partial z_{t,k}}{\partial \hat{z}_{t,j}} + \frac{\partial \log p(z_{t,k} | \mathbf{z}_{t-1})}{\partial z_{t,k}} \cdot \frac{\partial^2 z_{t,k}}{\partial \hat{z}_{t,i} \partial \hat{z}_{t,j}} \right) = 0 \quad (41)$$

Table 6: DMM-MAR Architecture details. BS: batch size, T: length of time series, $|\mathbf{x}_t|$: the dimension of \mathbf{x}_t .

Configuration	Description	Output
ϕ^A	Latent Variable Encoder	
Input: $\mathbf{x}_{1:T}^0$	Observed time series	Batch Size $\times T \times \mathbf{x}_t $
Dense	Conv1d	Batch Size $\times m \times \mathbf{x}_t $
Dense	Conv1d	Batch Size $\times T \times \mathbf{x}_t $
Dense	d neurons	Batch Size $\times T \times d$
F^A	Decoder	
Input: $\mathbf{z}_{1:T}, \mathbf{c}_{1:T}$	Latent Variable	Batch Size $\times T \times d$
Dense	$ \mathbf{x}_t $ neurons	Batch Size $\times T \times \mathbf{x}_t $
\mathbf{r}	Modular Prior Networks	
Input: $\mathbf{z}_{1:T}$ or $\mathbf{c}_{1:T}$	Latent Variable	Batch Size $\times (n+1)$
Dense	128 neurons, LeakyReLU	$(n+1) \times 128$
Dense	128 neurons, LeakyReLU	128×128
Dense	128 neurons, LeakyReLU	128×128
Dense	1 neuron	Batch Size $\times 1$
JacobianCompute	Compute $\log(\det(\mathbf{J}))$	Batch Size

For each value of \mathbf{z}_t , $\mathbf{v}_{t,k,l}^B - \mathbf{v}_{t,k,n}^B$ are linearly independent, so $\frac{\partial z_{t,k}}{\partial z_{t,i}} \cdot \frac{\partial z_{t,k}}{\partial z_{t,j}} = 0$. That is, in each row of \mathbf{J}_h^B there is only one non-zero entry. Since \mathbf{h} is invertible, then \mathbf{z}_t is component-wise identifiable.

Similarly, we have $p(h_c(\hat{\mathbf{c}}_t)) = p(\mathbf{c}_t)$, then

$$\log p(\hat{\mathbf{c}}_t | \mathbf{x}_{t-1}) = \log p(\mathbf{c}_t | \mathbf{x}_{t-1}) + \log |\mathbf{J}_{h_c}^B| = \sum_{k=1}^n \log p(c_{t,k} | \mathbf{x}_{t-1}) + \log |\mathbf{J}_{h_c}^B| \quad (42)$$

For $i, j \in \{1, \dots, n\}$, $i \neq j$, conditioned on \mathbf{x}_{t-1} each $c_{t,i}$ is independent of any other $c_{t,j}$, we have:

$$\frac{\partial^2 \log p(\hat{\mathbf{c}}_t | \mathbf{x}_{t-1})}{\partial \hat{c}_{t,i} \partial \hat{c}_{t,j}} = 0 \quad (43)$$

Sequentially, the first-order derivative w.r.t. $\hat{c}_{t,i}$ is

$$\frac{\partial \log p(\hat{\mathbf{c}}_t | \mathbf{x}_{t-1})}{\partial \hat{c}_{t,i}} = \sum_{k=1}^n \frac{\partial \log p(c_{t,k} | \mathbf{x}_{t-1})}{\partial c_{t,k}} \cdot \frac{\partial c_{t,k}}{\partial \hat{c}_{t,i}} + \frac{\partial \log |\mathbf{J}_{h_c}^B|}{\partial \hat{c}_{t,i}} \quad (44)$$

Sequentially, we conduct the second-order derivative w.r.t $\hat{c}_{t,j}, \hat{c}_{t,j}$ and have

$$\frac{\partial^2 \log p(\hat{\mathbf{c}}_t | \mathbf{x}_{t-1})}{\partial \hat{c}_{t,i} \partial \hat{c}_{t,j}} = \sum_{k=1}^n \left(\frac{\partial^2 \log p(c_{t,k} | \mathbf{x}_{t-1})}{\partial^2 c_{t,k}} \cdot \frac{\partial c_{t,k}}{\partial \hat{c}_{t,i}} \cdot \frac{\partial c_{t,k}}{\partial \hat{c}_{t,j}} + \frac{\partial \log p(c_{t,k} | \mathbf{x}_{t-1})}{\partial c_{t,k}} \cdot \frac{\partial^2 c_{t,k}}{\partial \hat{c}_{t,i} \partial \hat{c}_{t,j}} \right) + \frac{\partial^2 \log |\mathbf{J}_{h_c}^B|}{\partial \hat{c}_{t,i} \partial \hat{c}_{t,j}} \quad (45)$$

Therefore, there exist $2n+1$ values of \mathbf{x}_{t-1} , i.e., $\mathbf{x}_{t-1,l}$ with $j = 0, 2, \dots, 2n$, we have $2n+1$ such equations. Subtracting each equation corresponding to $\mathbf{x}_{t-1,1} \dots \mathbf{x}_{t-1,2n}$ with the equation corresponding to $\mathbf{x}_{t-1,0}$ results in $2n$ equations:

$$\begin{aligned} & \sum_{k=1}^n \left(\left(\frac{\partial^2 \log p(c_{t,k} | \mathbf{x}_{t-1,l})}{\partial^2 c_{t,k}} - \frac{\partial^2 \log p(c_{t,k} | \mathbf{x}_{t-1,0})}{\partial^2 c_{t,k}} \right) \cdot \frac{\partial c_{t,k}}{\partial \hat{c}_{t,i}} \cdot \frac{\partial c_{t,k}}{\partial \hat{c}_{t,j}} \right. \\ & \quad \left. + \left(\frac{\partial \log p(c_{t,k} | \mathbf{x}_{t-1,l})}{\partial c_{t,k}} - \frac{\partial \log p(c_{t,k} | \mathbf{x}_{t-1,0})}{\partial c_{t,k}} \right) \cdot \frac{\partial^2 c_{t,k}}{\partial \hat{c}_{t,i} \partial \hat{c}_{t,j}} \right) = 0 \end{aligned} \quad (46)$$

under the linear independence condition in Assumption A3, we have $\frac{\partial c_{t,k}}{\partial \hat{c}_{t,i}} \cdot \frac{\partial c_{t,k}}{\partial \hat{c}_{t,j}} = 0$. That is, in each row of $\mathbf{J}_{h_c}^B$ there is only one non-zero entry. Since h_c is invertible, then \mathbf{c}_t is component-wise identifiable. \square

D More Details on Missing mechanism

Since the missing mechanism in the imputation m-graph differs from the definition of standard m-graph [Mohan *et al.*, 2013], we give more detail illustration for them.

D.1 Missing At Random (MAR) in Imputation M-graphs

To better understand the data generation process of missing at random, we suppose that \mathbf{x}_t denotes the measurable index like blood pressure and blood glucose. And \mathbf{z}_t denotes the virus concentration. A doctor may find that the blood pressure is within the normal range and does not record the values of blood glucose, resulting in the missingness. In this case, the missing cause variables denote the doctor's willingness to conduct further examinations.

Table 7: DMM-MNAR Architecture details. BS: batch size, τ : Segment the T-length time series data into segments, with each segment being τ in length, $|\mathbf{x}_t|$: the dimension of \mathbf{x}_t .

Configuration	Description	Output
ϕ_z^B	Latent Variable Encoder	
Input: $\mathbf{x}_{t:t+\tau}^o$	Observed time series	Batch Size $\times \tau \times \mathbf{x}_t $
Dense	Conv1d	Batch Size $\times m \times \mathbf{x}_t $
Dense	Conv1d	Batch Size $\times \tau \times \mathbf{x}_t $
Dense	d neurons	Batch Size $\times \tau \times d$
ϕ_c^B	Latent Variable Encoder	
Input: $\mathbf{x}_{t-\tau:t-1}^o, \mathbf{x}_{t-\tau:t-1}^m$	Time series	Batch Size $\times \tau \times \mathbf{x}_t $
Dense	Conv1d	Batch Size $\times m \times \mathbf{x}_t $
Dense	Conv1d	Batch Size $\times \tau \times \mathbf{x}_t $
Dense	d neurons	Batch Size $\times \tau \times d$
F^B	Decoder	
Input: $\mathbf{z}_{t:t+\tau}, \mathbf{c}_{t:t+\tau}$	Latent Variable	Batch Size $\times \tau \times d$
Dense	$ \mathbf{x}_t $ neurons	Batch Size $\times \tau \times \mathbf{x}_t $
\mathbf{r}	Modular Prior Networks	
Input: $\mathbf{z}_{1:T}$ or $\mathbf{c}_{1:T}$	Latent Variable	Batch Size $\times (n+1)$
Dense	128 neurons, LeakyReLU	$(n+1) \times 128$
Dense	128 neurons, LeakyReLU	128×128
Dense	128 neurons, LeakyReLU	128×128
Dense	1 neuron	Batch Size $\times 1$
JacobianCompute	Compute $\log(\det(\mathbf{J}))$	Batch Size

D.2 Missing Not At Random (MNAR)

We also provide a medical example. When the examination indicators of a patient exceed the normal range, he may choose to discontinue treatment at this point, resulting in missing subsequent data. In this case, the missing cause denotes the patient's willingness to undergo further treatment.

D.3 Missing Completely At Random (MCAR)

When patients are unable to go to the hospital for testing in a timely manner due to work or personal reasons, resulting in missing indicators. This type of missing is not dependent on data, but is caused by completely random factors. In this case, the missing cause denotes that the unexpected situation did not occur and the patient went to the hospital for examination on time.

E Explanation of Assumptions

E.1 Discussion of the Identification Results

We would like to highlight that the theoretical results provide sufficient conditions for the identification of our model. That implies: 1) our model can be correctly identified when all the assumptions hold. 2) at the same time, even if some of the above assumptions do not hold, our method may still learn the correct model. From an application perspective, these assumptions rigorously defined a subset of applicable scenarios of our model. Thus, we provide detailed explanations of the assumptions, how they relate to real-world scenarios, and in which scenarios they are satisfied.

E.2 Smooth, Positive and Conditional independent Density.

This assumption is common in the existing identification results [Yao *et al.*, 2022; Yao *et al.*, 2021]. In real-world scenarios, smooth and positive density implies continuous changes in historical information, such as temperature variations in weather data. To achieve this, we should sample as much data as possible to learn the transition probabilities more accurately. Moreover, The conditional independent assumption is also common in identifying temporal latent processes [Li *et al.*, 2024a]. Intuitively, it means there are no immediate relations among latent variables. To satisfy this assumption, we can sample data at high frequency to avoid instantaneous dependencies caused by subsampling.

E.3 Linear Independence.

The second assumption is also common in [Kong *et al.*, 2022; Yao *et al.*, 2022], meaning that the influence from each latent source to observation is independent. The linear independence assumption is standard in the identification of nonlinear ICA [Allman *et al.*, 2009]. It implies that linear independence is necessary for a unique solution to a system of equations. Though this assumption is untestable, we may investigate whether it is satisfied through the prior knowledge of the applications.

F Implementation Details

E.1 Prior Likelihood Derivation

In this section, for the data generation process of MAR, we derive the prior of $p(\hat{\mathbf{z}}_{1:t})$ and $p(\hat{\mathbf{c}}_{1:t})$ as follows:

We first consider the prior of $\ln p(\mathbf{z}_{1:t})$. We start with an illustrative example of stationary latent causal processes with two time-delay latent variables, i.e. $\mathbf{z}_t = [z_{t,1}, z_{t,2}]$ with maximum time lag $L = 1$, i.e., $z_{t,i} = f_i^A(\mathbf{z}_{t-1}, \epsilon_{t,i}^z)$ with mutually independent noises. Then we write this latent process as a transformation map \mathbf{f}^A (note that we overload the notation f for transition functions and for the transformation map):

$$\begin{bmatrix} z_{t-1,1} \\ z_{t-1,2} \\ z_{t,1} \\ z_{t,2} \end{bmatrix} = \mathbf{f}^A \left(\begin{bmatrix} z_{t-1,1} \\ z_{t-1,2} \\ \epsilon_{t,1}^z \\ \epsilon_{t,2}^z \end{bmatrix} \right).$$

By applying the change of variables formula to the map \mathbf{f}^A , we can evaluate the joint distribution of the latent variables $p(z_{t-1,1}, z_{t-1,2}, z_{t,1}, z_{t,2})$ as

$$p(z_{t-1,1}, z_{t-1,2}, z_{t,1}, z_{t,2}) = \frac{p(z_{t-1,1}, z_{t-1,2}, \epsilon_{t,1}^z, \epsilon_{t,2}^z)}{|\det \mathbf{J}_{\mathbf{f}^A}|}, \quad (47)$$

where $\mathbf{J}_{\mathbf{f}^A}$ is the Jacobian matrix of the map \mathbf{f}^A , which is naturally a low-triangular matrix:

$$\mathbf{J}_{\mathbf{f}^A} = \begin{bmatrix} 1 & 0 & 0 & 0 \\ 0 & 1 & 0 & 0 \\ \frac{\partial z_{t,1}}{\partial z_{t-1,1}} & \frac{\partial z_{t,1}}{\partial z_{t-1,2}} & \frac{\partial z_{t,1}}{\partial \epsilon_{t,1}^z} & 0 \\ \frac{\partial z_{t,2}}{\partial z_{t-1,1}} & \frac{\partial z_{t,2}}{\partial z_{t-1,2}} & 0 & \frac{\partial z_{t,2}}{\partial \epsilon_{t,2}^z} \end{bmatrix}.$$

Given that this Jacobian is triangular, we can efficiently compute its determinant as $\prod_i \frac{\partial z_{t,i}}{\partial \epsilon_{t,i}^z}$. Furthermore, because the noise terms are mutually independent, and hence $\epsilon_{t,i}^z \perp \epsilon_{t,j}^z$ for $j \neq i$ and $\epsilon_t^z \perp \mathbf{z}_{t-1}$, so we can with the RHS of Equation (47) as follows

$$p(z_{t-1,1}, z_{t-1,2}, z_{t,1}, z_{t,2}) = p(z_{t-1,1}, z_{t-1,2}) \times \frac{p(\epsilon_{t,1}^z, \epsilon_{t,2}^z)}{|\mathbf{J}_{\mathbf{f}^A}|} = p(z_{t-1,1}, z_{t-1,2}) \times \frac{\prod_i p(\epsilon_{t,i}^z)}{|\mathbf{J}_{\mathbf{f}^A}|}. \quad (48)$$

Finally, we generalize this example and derive the prior likelihood below. Let $\{r_i^A\}_{i=1,2,3,\dots}$ be a set of learned inverse transition functions that take the estimated latent causal variables, and output the noise terms, i.e., $\hat{\epsilon}_{t,i}^z = r_i^A(\hat{z}_{t,i}, \{\hat{\mathbf{z}}_{t-\tau}\})$. Then we design a transformation $\mathbf{A} \rightarrow \mathbf{B}$ with low-triangular Jacobian as follows:

$$\underbrace{[\hat{\mathbf{z}}_{t-L}, \dots, \hat{\mathbf{z}}_{t-1}, \hat{\mathbf{z}}_t]^\top}_{\mathbf{A}} \text{ mapped to } \underbrace{[\hat{\mathbf{z}}_{t-L}, \dots, \hat{\mathbf{z}}_{t-1}, \hat{\epsilon}_{t,i}^z]^\top}_{\mathbf{B}}, \text{ with } \mathbf{J}_{\mathbf{A} \rightarrow \mathbf{B}} = \begin{bmatrix} \mathbb{I}_{n \times L} & 0 \\ * & \text{diag} \left(\frac{\partial r_i^A}{\partial \hat{z}_{t,i}} \right) \end{bmatrix}. \quad (49)$$

Similar to Equation (48), we can obtain the joint distribution of the estimated dynamics subspace as:

$$\ln p(\mathbf{A}) = \ln p(\hat{\mathbf{z}}_{t-L}, \dots, \hat{\mathbf{z}}_{t-1}) + \underbrace{\sum_{i=1}^n \ln p(\hat{\epsilon}_{t,i}^z) + \ln(|\det(\mathbf{J}_{\mathbf{A} \rightarrow \mathbf{B}})|)}_{\text{Because of mutually independent noise assumption}} \quad (50)$$

Finally, we have:

$$\ln p(\hat{\mathbf{z}}_t | \{\hat{\mathbf{z}}_{t-\tau}\}_{\tau=1}^L) = \sum_{i=1}^n \ln p(\hat{\epsilon}_{t,i}^z) + \sum_{i=1}^n \ln \left| \frac{\partial r_i^A}{\partial \hat{z}_{t,i}} \right| \quad (51)$$

Since the prior of $p(\hat{\mathbf{z}}_{t+1:T} | \hat{\mathbf{z}}_{1:t}) = \prod_{i=t+1}^T p(\hat{\mathbf{z}}_i | \hat{\mathbf{z}}_{i-1})$ with the assumption of first-order Markov assumption, we can estimate $p(\hat{\mathbf{z}}_{t+1:T} | \hat{\mathbf{z}}_{1:t})$ in a similar way. We then consider the prior of $\ln p(\hat{\mathbf{c}}_{1:t})$. Similar to the derivation of $\ln p(\hat{\mathbf{z}}_{1:t})$, we let $\{c_i\}_{i=1,2,3,\dots}$ be a set of learned inverse transition functions that take the estimated latent variables as input and output the noise terms, i.e. $\hat{\epsilon}_t^c = s_i^A(x_t^o, \hat{c}_{t,i})$. Similarly, we design a transformation $\mathbf{A} \rightarrow \mathbf{B}$ with low-triangular Jacobian as follows:

$$\underbrace{[\mathbf{x}_t^o, \hat{\mathbf{c}}_t]^\top}_{\mathbf{A}} \text{ mapped to } \underbrace{[\mathbf{x}_t^o, \hat{\epsilon}_t^c]^\top}_{\mathbf{B}}, \text{ with } \mathbf{J}_{\mathbf{A} \rightarrow \mathbf{B}} = \begin{bmatrix} \mathbb{I} & 0 \\ * & \text{diag} \left(\frac{\partial s_i^A}{\partial \hat{\mathbf{c}}_{t,i}} \right) \end{bmatrix}. \quad (52)$$

Since the noise $\hat{\epsilon}_t^c$ is independent of \mathbf{x}_t^o we have

$$\ln p(\hat{\mathbf{c}}_t | \mathbf{x}_t^o) = \ln p(\hat{\epsilon}_t^c) + \sum_{i=1}^n \ln \left| \frac{\partial s_i^A}{\partial \hat{c}_{t,i}} \right|. \quad (53)$$

Therefore, the missing cause prior can be estimated by maximizing the following equation, obtained by summing Equation (53) across time steps from 1 to t .

$$\ln p(\hat{\mathbf{c}}_{1:t} | x_{1:t}^o) = \sum_{\tau=1}^t \left(\sum_{i=1}^n \ln p(\hat{\epsilon}_{\tau,i}^c) + \sum_{i=1}^n \ln \left| \frac{\partial s_i^A}{\partial \hat{c}_{\tau,i}} \right| \right). \quad (54)$$

Similarly, for the data generation process of MNAR, we derive the prior of $p(\hat{\mathbf{z}}_{1:t})$ and $p(\hat{\mathbf{c}}_{1:t})$ as follows:

We first consider the prior of $\ln p(\mathbf{z}_{1:t})$. We start with an illustrative example of stationary latent causal processes with two time-delay latent variables, i.e. $\mathbf{z}_t = [z_{t,1}, z_{t,2}]$ with maximum time lag $L = 1$, i.e., $z_{t,i} = f_i^B(\mathbf{z}_{t-1}, \varepsilon_{t,i}^z)$ with mutually independent noises. Then we write this latent process as a transformation map \mathbf{f}^B (note that we overload the notation f for transition functions and for the transformation map):

$$\begin{bmatrix} z_{t-1,1} \\ z_{t-1,2} \\ z_{t,1} \\ z_{t,2} \end{bmatrix} = \mathbf{f}^B \left(\begin{bmatrix} z_{t-1,1} \\ z_{t-1,2} \\ \varepsilon_{t,1}^z \\ \varepsilon_{t,2}^z \end{bmatrix} \right).$$

By applying the change of variables formula to the map \mathbf{f}^B , we can evaluate the joint distribution of the latent variables $p(z_{t-1,1}, z_{t-1,2}, z_{t,1}, z_{t,2})$ as:

$$p(z_{t-1,1}, z_{t-1,2}, z_{t,1}, z_{t,2}) = \frac{p(z_{t-1,1}, z_{t-1,2}, \varepsilon_{t,1}^z, \varepsilon_{t,2}^z)}{|\det \mathbf{J}_{\mathbf{f}^B}|}, \quad (55)$$

where $\mathbf{J}_{\mathbf{f}^B}$ is the Jacobian matrix of the map \mathbf{f}^B , which is naturally a low-triangular matrix:

$$\mathbf{J}_{\mathbf{f}^B} = \begin{bmatrix} 1 & 0 & 0 & 0 \\ 0 & 1 & 0 & 0 \\ \frac{\partial z_{t,1}}{\partial z_{t-1,1}} & \frac{\partial z_{t,1}}{\partial z_{t-1,2}} & \frac{\partial z_{t,1}}{\partial \varepsilon_{t,1}^z} & 0 \\ \frac{\partial z_{t,2}}{\partial z_{t-1,1}} & \frac{\partial z_{t,2}}{\partial z_{t-1,2}} & 0 & \frac{\partial z_{t,2}}{\partial \varepsilon_{t,2}^z} \end{bmatrix}.$$

Given that this Jacobian is triangular, we can efficiently compute its determinant as $\prod_i \frac{\partial z_{t,i}}{\partial \varepsilon_{t,i}^z}$. Furthermore, because the noise terms are mutually independent, and hence $\varepsilon_{t,i}^z \perp \varepsilon_{t,j}^z$ for $j \neq i$ and $\varepsilon_t^z \perp \mathbf{z}_{t-1}$, so we can with the RHS of Equation (47) as follows

$$p(z_{t-1,1}, z_{t-1,2}, z_{t,1}, z_{t,2}) = p(z_{t-1,1}, z_{t-1,2}) \times \frac{p(\varepsilon_{t,1}^z, \varepsilon_{t,2}^z)}{|\mathbf{J}_{\mathbf{f}^B}|} = p(z_{t-1,1}, z_{t-1,2}) \times \frac{\prod_i p(\varepsilon_{t,i}^z)}{|\mathbf{J}_{\mathbf{f}^B}|}. \quad (56)$$

Finally, we generalize this example and derive the prior likelihood below. Let $\{r_i^B\}_{i=1,2,3,\dots}$ be a set of learned inverse transition functions that take the estimated latent causal variables, and output the noise terms, i.e., $\hat{\varepsilon}_{t,i}^z = r_i^B(\hat{z}_{t,i}, \{\hat{\mathbf{z}}_{t-\tau}\})$. Then we design a transformation $\mathbf{A} \rightarrow \mathbf{B}$ with low-triangular Jacobian as follows:

$$\underbrace{[\hat{\mathbf{z}}_{t-L}, \dots, \hat{\mathbf{z}}_{t-1}, \hat{\mathbf{z}}_t]^\top}_{\mathbf{A}} \text{ mapped to } \underbrace{[\hat{\mathbf{z}}_{t-L}, \dots, \hat{\mathbf{z}}_{t-1}, \hat{\varepsilon}_{t,i}^z]^\top}_{\mathbf{B}}, \text{ with } \mathbf{J}_{\mathbf{A} \rightarrow \mathbf{B}} = \begin{bmatrix} \mathbb{I}_{n \times L} & 0 \\ * & \text{diag} \left(\frac{\partial r_i^B}{\partial \hat{z}_{t,i}} \right) \end{bmatrix}. \quad (57)$$

Similar to Equation (48), we can obtain the joint distribution of the estimated dynamics subspace as:

$$\ln p(\mathbf{A}) = \ln p(\hat{\mathbf{z}}_{t-L}, \dots, \hat{\mathbf{z}}_{t-1}) + \underbrace{\sum_{i=1}^n \ln p(\hat{\varepsilon}_{t,i}^z)}_{\text{Because of mutually independent noise assumption}} + \ln(|\det(\mathbf{J}_{\mathbf{A} \rightarrow \mathbf{B}})|) \quad (58)$$

Finally, we have:

$$\ln p(\hat{\mathbf{z}}_t | \{\hat{\mathbf{z}}_{t-\tau}\}_{\tau=1}^L) = \sum_{i=1}^n \ln p(\hat{\varepsilon}_{t,i}^z) + \sum_{i=1}^n \ln \left| \frac{\partial r_i^B}{\partial \hat{z}_{t,i}} \right| \quad (59)$$

Since the prior of $p(\hat{\mathbf{z}}_{t+1:T}|\hat{\mathbf{z}}_{1:t}) = \prod_{i=t+1}^T p(\hat{\mathbf{z}}_i|\hat{\mathbf{z}}_{i-1})$ with the assumption of first-order Markov assumption, we can estimate $p(\hat{\mathbf{z}}_{t+1:T}|\hat{\mathbf{z}}_{1:t})$ in a similar way. We then consider the prior of $\ln p(\hat{\mathbf{c}}_{1:t})$. Similar to the derivation of $\ln p(\hat{\mathbf{z}}_{1:t})$, we let $\{c_i\}_{i=1,2,3,\dots}$ be a set of learned inverse transition functions that take the estimated latent variables as input and output the noise terms, i.e. $\hat{\varepsilon}_t^c = s_i^B(\mathbf{x}_{t-1}^o, \hat{\mathbf{x}}_{t-1}^m, \hat{c}_{t,i})$. Similarly, we design a transformation $\mathbf{A} \rightarrow \mathbf{B}$ with low-triangular Jacobian as follows:

$$\underbrace{[\mathbf{x}_{t-1}^o, \hat{\mathbf{x}}_{t-1}^m, \hat{c}_t]^\top}_{\mathbf{A}} \quad \text{mapped to} \quad \underbrace{[\mathbf{x}_{t-1}^o, \hat{\mathbf{x}}_{t-1}^m, \hat{\varepsilon}_t^c]^\top}_{\mathbf{B}}, \text{with} \quad \mathbf{J}_{\mathbf{A} \rightarrow \mathbf{B}} = \begin{bmatrix} \mathbb{I} & 0 \\ * & \text{diag}\left(\frac{\partial s_i^B}{\partial \hat{c}_{t,i}}\right) \end{bmatrix}. \quad (60)$$

Since the noise $\hat{\varepsilon}_t^c$ is independent of \mathbf{x}_t^o we have

$$\ln p(\hat{\mathbf{c}}_t|\mathbf{x}_{t-1}^o, \hat{\mathbf{x}}_{t-1}^m) = \ln p(\hat{\varepsilon}_t^c) + \sum_{i=1}^{n_c} \ln \left| \frac{\partial s_i^B}{\partial \hat{c}_{t,i}} \right|. \quad (61)$$

Therefore, the missing cause prior can be estimated by maximizing the following equation, obtained by summing Equation (61) across time steps from 1 to t.

$$\ln p(\hat{\mathbf{c}}_{1:t}|\mathbf{x}_{1:t-1}^o, \hat{\mathbf{x}}_{1:t-1}^m) = \ln p(\hat{\mathbf{c}}_1) + \sum_{\tau=2}^t \left(\sum_{i=1}^{n_c} \ln p(\hat{\varepsilon}_{\tau,i}^c) + \sum_{i=1}^{n_c} \ln \left| \frac{\partial s_i^B}{\partial \hat{c}_{\tau,i}} \right| \right). \quad (62)$$

F.2 Evident Lower Bound

In this subsection, we show the evident lower bound. For the data generation process of MAR, we have:

$$\begin{aligned} \ln p(x_{1:T}^m) &= \ln \frac{p(x_{1:T}^m, \mathbf{z}_{1:T}, \mathbf{c}_{1:T})q(\mathbf{z}_{1:T}, \mathbf{c}_{1:T}|x_{1:T}^o)}{p(\mathbf{z}_{1:T}, \mathbf{c}_{1:T}|x_{1:T}^m)q(\mathbf{z}_{1:T}, \mathbf{c}_{1:T}|x_{1:T}^o)} \geq \ln \frac{p(x_{1:T}^m, \mathbf{z}_{1:T}, \mathbf{c}_{1:T})}{q(\mathbf{z}_{1:T}, \mathbf{c}_{1:T}|x_{1:T}^o)} = \ln \frac{p(x_{1:T}^m|\mathbf{z}_{1:T}, \mathbf{c}_{1:T})p(\mathbf{c}_{1:T}|\mathbf{z}_{1:T})p(\mathbf{z}_{1:T})}{q(\mathbf{z}_{1:T}|x_{1:T}^o)q(\mathbf{c}_{1:T}|x_{1:T}^o)} \\ &= \underbrace{\mathbb{E}_{q(\mathbf{z}_{1:T}, \mathbf{c}_{1:T}|\mathbf{x}_{1:T}^o)} \ln p(\mathbf{x}_{1:T}^m|\mathbf{z}_{1:T}, \mathbf{c}_{1:T})}_{\mathcal{L}_R} - \underbrace{D_{KL}(q(\mathbf{z}_{1:T}|\mathbf{x}_{1:T}^o)||p(\mathbf{z}_{1:T}))}_{\mathcal{L}_K^z} - \underbrace{D_{KL}(q(\mathbf{c}_{1:T}|\mathbf{x}_{1:T}^o)||p(\mathbf{c}_{1:T}|\mathbf{z}_{1:T}))}_{\mathcal{L}_K^c}, \end{aligned} \quad (63)$$

Similar to the DMM-MAR model, we employ the variational inference to model the data generation process of the MNAR mechanism, and the ELBO is

$$\begin{aligned} \ln p(x_{1:T}^m) &= \ln \frac{p(x_{1:T}^m, \mathbf{z}_{1:T}, \mathbf{c}_{1:T})}{p(\mathbf{z}_{1:T}, \mathbf{c}_{1:T}|x_{1:T}^m)} \geq \ln \frac{p(x_{1:T}^m, \mathbf{z}_{1:T}, \mathbf{c}_{1:T})}{q(\mathbf{z}_{1:T}|x_{1:T}^o)q(\mathbf{c}_{1:T}|x_{1:T-1})} = \ln \frac{p(x_{1:T}^m|\mathbf{z}_{1:T}, \mathbf{c}_{1:T})p(\mathbf{c}_{1:T}|\mathbf{z}_{1:T})p(\mathbf{z}_{1:T})}{q(\mathbf{z}_{1:T}|x_{1:T}^o)q(\mathbf{c}_{1:T}|x_{1:T-1})} \\ &= \underbrace{\mathbb{E}_{q(\mathbf{z}_{1:T}, \mathbf{c}_{1:T}|\mathbf{x}_{1:T}^o)} \ln p(\mathbf{x}_{1:T}^m|\mathbf{z}_{1:T}, \mathbf{c}_{1:T})}_{\mathcal{L}_R} - \underbrace{D_{KL}(q(\mathbf{z}_{1:T}|\mathbf{x}_{1:T}^o)||p(\mathbf{z}_{1:T}))}_{\mathcal{L}_K^z} - \underbrace{D_{KL}(q(\mathbf{c}_{1:T}|\mathbf{x}_{1:T-1})||p(\mathbf{c}_{1:T}|\mathbf{z}_{1:T}))}_{\mathcal{L}_K^c}, \end{aligned} \quad (64)$$

F.3 Model Details

We choose CNN as the encoder backbone of our model on real-world datasets. Specifically, given the CNN extract the hidden feature, we apply a variational inference block and then a MLP-based decoder. Architecture details of the proposed method are shown in Table 6 and Table 7.

G Limitation

One limitation of our method is the invertible mixing process. In a few real-world applications, certain violations of the assumption can be discernible to a certain degree, such as occlusion and visual persistence in videos. For example, when an object is blocked by another, it is improbable to completely recover the corresponding latent variable from the observation. Moreover, the blur resulting from high - speed moving objects can be regarded as a mixing process that combines latent variables from different time steps, thus further causing non-invertibility. By circumventing such cases, the assumption can be ensured to some extent. Even if the assumption fails to hold, there remain potential approaches for identifying latent causal structures. For example, recent work [Chen *et al.*, 2024] indicates that contextual information can be harnessed to regain the information lost as a result of the non-invertible mixing process. Since this method is orthogonal to the contributions of this paper, we did not incorporate this method into our approach.

Dataset	Ratio	DMM_MAR		DMM_MNAR		TimeCIB		ImputeFormer		TimesNet		SAITS		GPVAE		CSDI		BRITS		SSGAN	
		MSE	MAE	MSE	MAE	MSE	MAE	MSE	MAE	MSE	MAE	MSE	MAE	MSE	MAE	MSE	MAE	MSE	MAE	MSE	MAE
ETTh1	0.2	0.003	0.002	0.012	0.013	0.012	0.005	0.015	0.008	0.034	0.014	0.023	0.022	0.025	0.013	0.017	0.003	0.007	0.004	0.001	0.001
	0.4	0.019	0.014	0.036	0.012	0.004	0.001	0.011	0.014	0.028	0.011	0.033	0.014	0.023	0.014	0.003	0.001	0.008	0.005	0.012	0.009
	0.6	0.002	0.009	0.010	0.006	0.008	0.009	0.016	0.016	0.036	0.018	0.017	0.007	0.028	0.013	0.005	0.001	0.008	0.011	0.011	0.008
ETTh2	0.2	0.004	0.001	0.009	0.004	0.136	0.064	0.035	0.022	0.120	0.016	0.042	0.024	0.030	0.005	0.494	0.092	0.018	0.016	0.058	0.042
	0.4	0.005	0.003	0.008	0.006	0.032	0.019	0.022	0.010	0.260	0.049	0.023	0.013	0.033	0.008	0.031	0.013	0.039	0.021	0.010	0.013
	0.6	0.006	0.001	0.005	0.001	0.107	0.053	0.056	0.017	0.168	0.042	0.022	0.006	0.059	0.006	0.079	0.030	0.093	0.059	0.062	0.037
ETTm1	0.2	0.008	0.003	0.017	0.006	0.001	0.008	0.009	0.009	0.008	0.005	0.012	0.004	0.038	0.015	0.023	0.004	0.001	0.001	0.001	0.004
	0.4	0.009	0.003	0.023	0.008	0.001	0.004	0.025	0.017	0.059	0.016	0.005	0.006	0.037	0.016	0.012	0.002	0.002	0.003	0.006	0.003
	0.6	0.019	0.006	0.013	0.004	0.008	0.005	0.014	0.007	0.048	0.014	0.013	0.012	0.036	0.016	0.512	0.221	0.004	0.007	0.013	0.010
ETTm2	0.2	0.012	0.007	0.002	0.001	0.079	0.064	0.015	0.009	0.164	0.027	0.030	0.018	0.086	0.013	0.075	0.037	0.005	0.010	0.005	0.012
	0.4	0.007	0.014	0.005	0.002	0.004	0.006	0.025	0.012	0.159	0.032	0.039	0.020	0.058	0.006	0.002	0.001	0.025	0.025	0.025	0.027
	0.6	0.022	0.009	0.018	0.007	0.061	0.035	0.021	0.018	0.226	0.046	0.036	0.021	0.058	0.006	0.003	0.004	0.018	0.025	0.025	0.025
Exchange	0.2	0.018	0.022	0.013	0.005	0.079	0.024	0.012	0.003	0.081	0.011	0.044	0.035	0.111	0.027	0.061	0.039	0.035	0.026	0.073	0.051
	0.4	0.010	0.004	0.011	0.005	0.102	0.041	0.019	0.012	0.056	0.011	0.002	0.023	0.006	0.131	0.045	0.047	0.021	0.038	0.040	
	0.6	0.008	0.001	0.009	0.003	0.057	0.024	0.008	0.012	0.158	0.032	0.051	0.042	0.079	0.022	0.152	0.064	0.045	0.028	0.209	0.082
Weather	0.2	0.003	0.002	0.003	0.004	0.001	0.001	0.004	0.003	0.015	0.006	0.004	0.001	0.012	0.009	0.005	0.001	0.001	0.004	0.001	0.001
	0.4	0.003	0.013	0.002	0.001	0.003	0.007	0.005	0.001	0.050	0.015	0.005	0.002	0.012	0.008	0.001	0.001	0.002	0.004	0.003	0.005
	0.6	0.016	0.020	0.004	0.001	0.002	0.002	0.007	0.003	0.035	0.011	0.004	0.005	0.010	0.008	0.002	0.001	0.001	0.003	0.002	0.002

Table 8: The standard deviation in supervised scenarios for various datasets with different missing ratios under MAR conditions.

Dataset	Ratio	DMM_MAR		DMM_MNAR		TimeCIB		ImputeFormer		TimesNet		SAITS		GPVAE		CSDI		BRITS		SSGAN	
		MSE	MAE	MSE	MAE	MSE	MAE	MSE	MAE	MSE	MAE	MSE	MAE	MSE	MAE	MSE	MAE	MSE	MAE	MSE	MAE
ETTh1	0.2	0.006	0.005	0.026	0.012	0.007	0.006	0.021	0.002	0.053	0.012	0.049	0.019	0.040	0.019	0.008	0.006	0.004	0.003	0.020	0.017
	0.4	0.003	0.001	0.009	0.004	0.007	0.007	0.011	0.003	0.016	0.009	0.036	0.011	0.044	0.020	0.022	0.019	0.012	0.013	0.024	0.004
	0.6	0.006	0.010	0.051	0.015	0.020	0.019	0.013	0.010	0.013	0.007	0.019	0.008	0.037	0.018	0.006	0.010	0.007	0.011	0.019	
ETTh2	0.2	0.026	0.011	0.033	0.014	0.124	0.066	0.033	0.007	0.161	0.037	0.011	0.015	0.015	0.009	0.019	0.011	0.061	0.048	0.024	0.015
	0.4	0.012	0.003	0.010	0.002	0.047	0.023	0.037	0.030	0.290	0.050	0.057	0.035	0.040	0.005	0.108	0.048	0.053	0.046	0.106	0.078
	0.6	0.006	0.002	0.008	0.001	0.131	0.071	0.015	0.009	0.029	0.016	0.109	0.045	0.044	0.004	0.171	0.099	0.078	0.056	0.118	0.074
ETTm1	0.2	0.002	0.001	0.026	0.019	0.002	0.003	0.022	0.015	0.026	0.003	0.013	0.004	0.039	0.018	0.003	0.004	0.001	0.002	0.003	0.006
	0.4	0.011	0.008	0.005	0.002	0.003	0.005	0.016	0.010	0.057	0.010	0.010	0.004	0.037	0.015	0.004	0.004	0.002	0.002	0.002	0.005
	0.6	0.032	0.016	0.002	0.006	0.004	0.005	0.017	0.015	0.058	0.015	0.013	0.002	0.042	0.017	0.002	0.001	0.004	0.003	0.003	0.002
ETTm2	0.2	0.010	0.004	0.001	0.002	0.044	0.047	0.020	0.010	0.038	0.014	0.011	0.013	0.043	0.002	0.169	0.010	0.010	0.016	0.017	0.022
	0.4	0.001	0.012	0.006	0.002	0.068	0.037	0.005	0.006	0.056	0.008	0.028	0.009	0.040	0.004	0.123	0.073	0.011	0.009	0.011	0.013
	0.6	0.007	0.001	0.007	0.001	0.065	0.046	0.030	0.007	0.030	0.003	0.0173	0.010	0.031	0.005	0.072	0.037	0.003	0.004	0.048	0.042
Exchange	0.2	0.001	0.001	0.003	0.002	0.113	0.039	0.004	0.009	0.164	0.035	0.039	0.030	0.046	0.012	0.042	0.016	0.063	0.051	0.043	0.037
	0.4	0.010	0.018	0.003	0.001	0.107	0.042	0.021	0.021	0.170	0.035	0.067	0.043	0.076	0.021	0.070	0.037	0.038	0.025	0.067	0.047
	0.6	0.042	0.010	0.043	0.012	0.083	0.034	0.020	0.020	0.373	0.083	0.063	0.042	0.070	0.020	0.051	0.026	0.009	0.001	0.016	0.001
Weather	0.2	0.002	0.005	0.023	0.042	0.001	0.002	0.002	0.001	0.022	0.008	0.003	0.001	0.014	0.008	0.002	0.001	0.003	0.004	0.001	0.002
	0.4	0.006	0.002	0.023	0.044	0.003	0.004	0.006	0.001	0.010	0.002	0.002	0.001	0.010	0.008	0.001	0.001	0.003	0.005	0.002	0.001
	0.6	0.001	0.002	0.023	0.038	0.003	0.003	0.006	0.002	0.004	0.001	0.003	0.001	0.004	0.002	0.001	0.002	0.003	0.004	0.001	0.002

Table 9: The standard deviation in supervised scenarios for various datasets with different missing ratios under MNAR conditions.

Dataset	Ratio	DMM_MAR		DMM_MNAR		TimeCIB		ImputeFormer		TimesNet		SAITS		GPVAE		CSDI		BRITS		SSGAN	
		MSE	MAE	MSE	MAE	MSE	MAE	MSE	MAE	MSE	MAE	MSE	MAE	MSE	MAE	MSE	MAE	MSE	MAE	MSE	MAE
ETTh1	0.2	0.009	0.006	0.007	0.010	0.026	0.010	0.132	0.074	0.015	0.009	0.090	0.084	0.035	0.029	0.030	0.014	0.007	0.008	0.004	0.003
	0.4	0.005	0.011	0.009	0.016	0.024	0.007	0.085	0.038	0.010	0.010	0.126	0.091	0.028	0.133	0.024	0.008	0.012	0.013	0.010	0.014
	0.6	0.014	0.002	0.006	0.01																

Dataset		A-MAR						A-MNAR											
Ratio		0.2			0.4			0.6			0.2			0.4			0.6		
DMM_MAR		0.939			0.920			0.937			0.865			0.842			0.801		
DMM_MNAR		0.891			0.879			0.868			0.960			0.869			0.855		

Table 12: Experiments results of MCC on missing cause variable c .

Dataset	Ratio	DMM-MAR	DMM-MNAR	TimeCIB	ImputeFormer	TimesNet	SAITS	GPVAE	CSDI	BRITS	SSGAN
		MSE	MAE	MSE	MAE	MSE	MAE	MSE	MAE	MSE	MAE
Exchange	0.2	0.004	0.042	0.003	0.037	0.468	0.381	0.130	0.242	0.006	0.049
	0.4	0.008	0.062	0.006	0.046	0.479	0.427	0.078	0.194	0.011	0.064
	0.6	0.011	0.076	0.008	0.061	0.516	0.453	0.117	0.232	0.018	0.086

Table 13: Experiment results for Exchange datasets in unsupervised scenarios with the future time-step influence under MNAR conditions.

		Parameter				0	0.0001	0.001	0.01	0.1
z_weight	A-MAR	DMM-MAR		0.871	0.880	0.910	0.913	0.905		
		DMM-MNAR		0.866	0.879	0.887	0.878	0.872		
	A-MNAR	DMM-MAR		0.860	0.869	0.870	0.864	0.874		
		DMM-MNAR		0.899	0.915	0.917	0.911	0.908		
c_weight	A-MAR	DMM-MAR		0.872	0.894	0.910	0.906	0.892		
		DMM-MNAR		0.869	0.874	0.887	0.868	0.863		
	A-MNAR	DMM-MAR		0.864	0.871	0.870	0.875	0.868		
		DMM-MNAR		0.893	0.909	0.917	0.912	0.902		

Table 14: Sensitivity analysis of prior parameters of temporal latent variables z and missing cause variables c under missing rate of 0.4.

Dataset	Ratio	DMM-MAR	DMM-MNAR	TimeCIB	ImputeFormer	TimesNet	SAITS	GPVAE	CSDI	BRITS	SSGAN
		MSE	MAE	MSE	MAE	MSE	MAE	MSE	MAE	MSE	MAE
MIMIC-III	0.2	0.018	0.179	0.012	0.123	0.028	0.221	0.040	0.336	0.016	0.142
	0.4	0.014	0.167	0.013	0.155	0.033	0.241	0.040	0.346	0.016	0.184
	0.6	0.027	0.271	0.018	0.189	0.035	0.252	0.043	0.339	0.022	0.225

Table 15: Experiment results (Magnified 10-fold) in unsupervised scenarios for MIMIC with different missing ratios under MNAR conditions.

Mix_Ratio	Mask_Ratio	DMM-MAR	DMM-MNAR	TimeCIB	ImputeFormer	TimesNet	SAITS	GPVAE	CSDI	BRITS	SSGAN
		MSE	MAE	MSE	MAE	MSE	MAE	MSE	MAE	MSE	MAE
2:1:1	0.2	0.006	0.038	0.008	0.045	0.318	0.258	0.130	0.248	0.007	0.042
	0.4	0.009	0.061	0.010	0.068	0.409	0.285	0.058	0.180	0.008	0.057
	0.6	0.021	0.098	0.023	0.102	0.523	0.389	0.186	0.283	0.018	0.087
1:2:1	0.2	0.003	0.041	0.004	0.043	0.356	0.311	0.082	0.203	0.007	0.053
	0.4	0.008	0.055	0.010	0.062	0.480	0.353	0.060	0.178	0.020	0.087
	0.6	0.010	0.067	0.094	0.225	0.531	0.407	0.139	0.270	0.021	0.096
1:1:2	0.2	0.004	0.052	0.003	0.039	0.375	0.474	0.106	0.228	0.006	0.048
	0.4	0.008	0.061	0.006	0.052	0.608	0.545	0.129	0.249	0.015	0.078
	0.6	0.015	0.076	0.013	0.070	0.628	0.563	0.199	0.302	0.024	0.092
1:1:1	0.2	0.003	0.040	0.004	0.047	0.325	0.269	0.082	0.210	0.007	0.052
	0.4	0.007	0.056	0.010	0.067	0.453	0.325	0.098	0.226	0.019	0.086
	0.6	0.012	0.068	0.019	0.091	0.558	0.409	0.113	0.231	0.019	0.091

Table 16: Experiment results in unsupervised scenarios for Exchange dataset under a mixture of different missing mechanisms.